CATÓLICA

UNIVERSIDADE CATÓLICA PORTUGUESA | PORTO

Escola Superior de Biotecnologia

PORTABLE SENSOR FOR IMPEDANCE ANALYSIS IN FRUIT

by

Sofia Machado Magalhães

September 2016

September 2016

CATÓLICA
UNIVERSIDADE CATÓLICA PORTUGUESA | PORTO
Escola Superior de Biotecnologia

PORTABLE SENSOR FOR IMPEDANCE ANALYSIS IN FRUIT

Thesis presented to *Escola Superior de Biotecnologia* of the *Universidade Católica Portuguesa* to fulfil the requirements of Master of Science degree in Food Engineering

by
Sofia Machado Magalhães

Place: Escola Superior de Biotecnologia, Universidade Católica Portuguesa

Supervision: Prof. António César Ferreira;
Co-supervision: Prof. Miguel Velhote Correia

Resumo

A espectroscopia de impedância elétrica (EIS) é um método cuja aplicação na área da qualidade dos alimentos tem vindo a desenvolver-se. Diversos estudos demonstram que medições de impedância elétrica refletem alterações físicas nos alimentos. Nos últimos anos tem sido crescente a procura de novas técnicas para medição da qualidade dos alimentos. Contudo, algumas destas técnicas, tal como a espectroscopia de infravermelho, ou cromatografia gasosa, necessitam de equipamentos muito caros e de condições de medições especificas (laboratórios). A EIS utiliza equipamentos mais económicos, as medições podem ser realizadas em qualquer lugar (equipamentos portáteis), e são não invasivas. Na literatura é possível encontrar trabalhos com a aplicação do EIS em frutos, no entanto, a relação entre as propriedades dielétricas dos fruitos e o seu perfil metabólico ainda não foi totalmente explorado.

Esta dissertação tem como objetivo investigar as propriedades elétricas dos frutos e relacionar com critérios de qualidade. Foi utilizado um sistema integrado de EIS, EVAL-AD5933, que opera a partir de um computador com o software da Analog Devices. A presente dissertação descreve medições de impedância em frutos, realizados durante o processo de amadurecimento. Os resultados deste trabalho indicam o elevado potencial da EIS para futuras aplicações no campo. Foi realizada a calibração do sensor e estudos de fiabilidade do sistema. Procedeu-se a um pré-processamento aos espectros de impedância através do software Unscrambler, incluindo técnicas de análise multivariada, que permitiram a redução do elevado volume de dados a um conjunto de variáveis que descrevem a variabilidade das amostras. Para validar os resultados obtidos foi construído um modelo que relaciona os valores de impedância das uvas com o respetivo brixº através de um PLS (Partial Least Square).

Durante os testes realizados com o sensor foi possivel concluir que as propriedades electricas dos fruitos permitem a sua caracterização tanto ao nível da espécie de fruto como do seu estado de maturação. Também foi possivel criar um modelo de previsão de Brixº nas uvas a partir dos espectros de impedancia.

Os resultados demonstram que este sistema é promissor, com viabilidade para o desenvolvimento de futuros dispositivos com grande potencial para monitorizar o relógio metabólico dos frutos.

Abstract

Electrical impedance spectroscopy (EIS) is a relatively new method applied to food quality assessment. It has been demonstrated that impedance measurement is capable of reflecting rapid changes when the food has any physical damage, such as chilling and bruising. Numerous studies have been made to devise accurate food quality measuring techniques. However, some of the new techniques, such as infra-red spectroscopy, or gas chromatography have expensive equipment and strict experimental environment requirements. In contrast, EIS allows relatively (1 order of magnitude) inexpensive assessment, is fast, easy to operate and non-invasive. It has been adopted for investigation of fundamental electrical properties of fruits. However, the sensors applied are laboratory equipment without viability in an industrial context or in the field. The applications of EIS for fruit analysis have been reported previously, the analytically relationships between electrical impedance properties and metabolic properties of the fruit have not yet been fully developed and more importantly the ability to classify fruits during the ripping process was not yet fully explored.

This dissertation aims to investigate the electrical impedance properties of fruits and vegetables, and explore the relationship between impedance and quality criteria. It gives a description of a prototype impedance system based on the integrate system AD5933, which operates from a PC, with a software from “Analog Devices”.

In particular, the present dissertation outlines experimental research conducted the impedance changes observed during ripening process. With the correct system calibration measurements on different fruits have been performed with results which clearly demonstrate the high potential of the technique for future applications on the field. The research was also devoted on the sensor calibration as well as system reliability. Statistical processing of the results using both, analise of variance (ANOVA) and signal processing techniques using multivariate data analysis, enable the differentiating types of fruits and stages of maturation.

The results demonstrate that this system is a very promising technique, with exciting viability for further development to mobile devices suited to at line monitor the fruit quality has a great potential in assessing fruit ripening.

Acknowledgements

I would like to thank all the people who contributed in some way to the work described in this thesis. First and foremost, I wish to thank my academic advisor, Professor António César Ferreira. He has supported me not only by providing a research assistantship over all year, through the road to finish this thesis, thanks to him I had the opportunity to build a sensor. I greatly benefit from his scientific knowledge, his ability for solving difficulties and to put complex ideas into simple terms. Additionally, I would like to thank to Professor Miguel Velhote Correia for help me with the electronic aspects of my thesis, without his efforts my job would have undoubtedly been more difficult. Finally, I would like to acknowledge friends and family who supported me. Francisco help me with his friendship and unconditional support.

Contents:

Table of figures

Table of tables

1 Introduction

1.1 Context and motivation

Fifty percent of all fruits and vegetables in Europen Union go to waste, says a new report by the Food and Agriculture Organization (FAO) [Nadia Arumugam, "UN Says Europe Wastes 50% Of Fruit and Vegetables - And America Isn't Much Better.", 2012]. These losses occur throughout the entire food chain, from “farm to fork”. Accidental damage during threshing or fruit picking; damage by insects; mechanical damage and spillage during harvest, and crops filtered out by quality requirements of supermarkets and food companies are some of the reasons why 20% of the produce in Europe not even go to a grocery store. A report published by the European Commission at the end of 2011 revealed that up to 50% of all “edible and healthy” foods get wasted in EU households, eateries, supermarkets and along the food supply chain each year. Consumers expectations of higher food quality have risen along with improved standard of living. Therefore, it is great importance to develop effective food quality assessment techniques [Xing Liu, 2006]. Fruits are essentially required to be properly ripened to ensure about the development of all the nutrients. As the proper ripening of fruits conforms the maximum nutritional potential of the fruit, the under ripening and the over ripening are not desirable. Therefore, the ripening process of the fruits need to be studied, to eat the fruits when the best nutrients are available. Chemical and biochemical analysis can be conducted to study and evaluate the ripening state and the corresponding fruit quality, but these methods are destructive and takes a lot of time [Chowdhury et al., 2015]. To help combat those losses I propose a sensor that could help the farmers, grocers and food distributors better monitor their produce. The sensor can reveal the content of ripeness, in that way, grocers would know when to put certain items on sale to move them before they get too ripe. Electrical impedance measurement has been gain popularity for plant tissue investigations since 1800s, it is becoming more used to investigate the fundamental electrical properties of plant tissues and to detect tissue changes under different physiological conditions [Liu, 2006]. Fruit and vegetables are rich in metal ions and contain a big percentage of water. Thus, they are good electrical conductors and it is possible to perform impedance measurements on them. Since EI spectroscopy measurement allow cellular analysis towards fruits tissues, it is expected that impedance measurement can be used to monitor fruit changes during the time. The simple measurement of the electrical impedance together with advanced mathematical modeling is a good approach in quality assessment of agricultural products [Pliquett, 2010]. The increasing interest in sustainable and high-quality production in agricultural and food industries has promoted the development of more automated and precise monitoring analytically systems. Optimized process control tools are contributing to address the food safety rules of the end product and maintain the commercial viability of the business. Also, in the modern wine industry there is a strong need for timely information that can be used for grape berry maturity assessment, identification of the vineyard sections that should be segregated, and load quality assessment when grapes are delivered to the winery [D. Cozzolino,2011]. Since it is important the continuous study of the

application of electrical impedance techniques on food quality assessment, this thesis will propose a new sensor for impedance measurements on fresh fruit, and new approaches for quality determination. This sensor will be cheap, require almost no energy and can function at ambient temperatures, allowing the use in different environments.

1.2 Objectives of research

The objective of this research is to investigate the electrical impedance properties of fruits, and to propose new methods for fruit caracterization.

First, is presented a backgroung theory of electronics and impedance.

Secondly, this research aims to test the integrate circuit to improve the accuracy and stability of the system.

Thirdly, will study the aplicability of portable bio impedance sensor in fruit caracterization.

1.3 Background

In order to understand the essence of impedance, elements in passive electrical circuits should be described. Passive circuit elements are componets that do not generate current or potential in a passive electrical circuit. Three passive circuit elements will be described in this section.

1.3.1 Resistors

Resistance is the opposition to current flow around an electrical circuit. The unit of resistance is ohm. Resistors can also be connected together in various series and parallel combinations to form resistor networks which can act as voltage droppers, voltage dividers or current limiters within a circuit [Lessons in Electric Circuits].

“Ohm’s law states that the voltage V, across a resistor R, is directly proportional to the current I, flowing through the same resistor”.

$$I = \frac{V}{R}$$ Equation 1.1

- I: Current.
- V: Voltage.
- R: Resistance.

Figure 1.1 Resistor in a circuit

1.3.2 Capacitors

Capacitor is a simple passive device that is used to “store electricity”. The capacitor is a component which has the ability or “capacity” to store energy in the form of an electrical charge producing a potential difference (Static Voltage) across its plates. Capacitor consists of two or more parallel conductive (metal) plates which are not connected or touching each other, but are electrically separated either by air or by some form of a good insulating material or a liquid gel, used in electrolytic capacitors. The insulating layer between a capacitors plates is commonly called the dielectric. The capacitance value, C of a capacitor is an expression of the ratio between the amount of charge flowing and the rate of voltage change across the capacitor plates [Lessons in Electric Circuits].

$$C = \frac{Q}{V}$$ Equation 1.2

- C: farads
- Q: Coulombs
- V: Volts

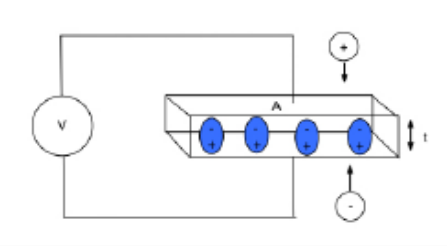

Figure 1.2 Parallel plate capacitor.

1.3.3 Inductors

The inductor is another device which is capable of storing charge and in its simplest form is a coil of wire.

Figure 1.3 Inductor in a circuit.

When a current is passed through the wire the flow of charge around the loops creates a strong electromagnetic field. The magnitude of this field is related to the total current flowing, an increase in the current increases the magnitude of the field, correspondingly a decrease in the current decreases the field. When an oscillating current passed through the inductor this creates a changing electromagnetic field and this in turn creates an induced voltage. This can be represented mathematically as $V_{induced} = L(\frac{di}{dt})$ where (L) is the inductance in Henry´s (H) [Resistors and Capacitors in Parallel].

1.3.4 Phase difference and phase shift

Comparing a voltage waveform with a current waveform, this produces an angular shift or phase difference between the two sinusoidal wave-forms. Phase shift is the lateral difference between two or more wave-forms along a common axis and sinusoidal wave-forms of the same frequency can have a phase difference [Basic Electronics Tutorials].

The excitation signal, expressed as a function of time has the form

$$E_t = E_0 \cos(\omega t + \varphi) \quad \text{Equation 1.3}$$

$$E_t = \omega E_0 \sin(\omega t + \varphi) \quad \text{Equation 1.4}$$

$$E_t = \omega E_0 \cos(\omega t + \varphi + \frac{\pi}{2}) \quad \text{Equation 1.5}$$

- Et: Potential time
- E_0: Amplitude of the signal
- ω: Radial frequency ($\omega = 2\pi f$).

In a linear system, the response signal, I_t, is shifted in phase (θ) and has a different amplitude, I_0, as $I_t = I_0 \sin(\omega t + \theta)$. Thus,

$$Z = \frac{E_t}{I_t} = \frac{E_0 \, sin(wt)}{I_0 \, sin(wt+\theta)} = Z_0 \frac{sin(wt)}{sin(wt+\theta)} \quad \text{Equation 1.6}$$

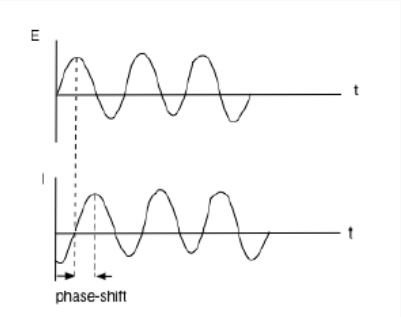

Figure 1.4 Sinusoidal current response in a linear system.

1.3.5 Impedance theory

Impedance Z, is the opposition to sinusoidal current flow in an AC circuit being the phasor sum of both reactance, X and resistance R. Z can change with frequency, temperature, orientation, mixture, pressure and molecular structure of the material. Impedance is an important parameter used to characterize electronic circuits, components, and the materials used to make components. Electrochemical impedance is usually measured by applying an AC potential to an electrochemical cell

and measuring the current through the cell. When applied a sinusoidal potential excitation, the response to this potential is an AC current signal. This current signal can be analyzed as a sum of sinusoidal functions, reactance X, and the resistance R. Although impedance represents the ratio of two phasors, it is not a phasor itself, because it does not correspond to a sinusoidal varying quantity [Liu, 2006].

Alternating current, or AC whose voltage switches polarity from positive to negative and back again over time the oscillating shape of an AC supply follows the mathematical form of a “sine wave” which is commonly called a sinusoidal waveform. Therefore, a sinusoidal voltage can be decribed by $V_{max}\sin(\omega t)$.

1.3.5.1 AC Resistance and impedance

Resistors convert electrical energy into heat. In DC circuits, the linear ratio of voltage to current in a resistor is called resistance. However, in AC circuits this ratio of voltage to current depends upon the frequency and phase difference, or phase angle, of the supply. The current flowing through the resistance is directly proportional to the voltage across it, with this linear relationship in an AC circuit being called Impedance. Impedance, which is given the letter Z, in a pure ohmic resistance is a complex number consisting only of a real part being the actual AC resistance value (R), and a zero imaginary part (j0). Because of this Ohm’s Law can be used in circuits containing an AC resistance to calculate these voltages and currents. For a purely resistive circuit the alternating current flowing through the resistor varies in proportion to the applied voltage across it following the same sinusoidal pattern. In a pure ohmic AC resistance, the current and voltage are both “in-phase” as there is no phase difference between them. As the supply frequency is common to both the voltage and current, their phasors will also be common resulting in the current being “in-phase” with the voltage, ($\theta = 0$) [Basic Electronics Tutorials].

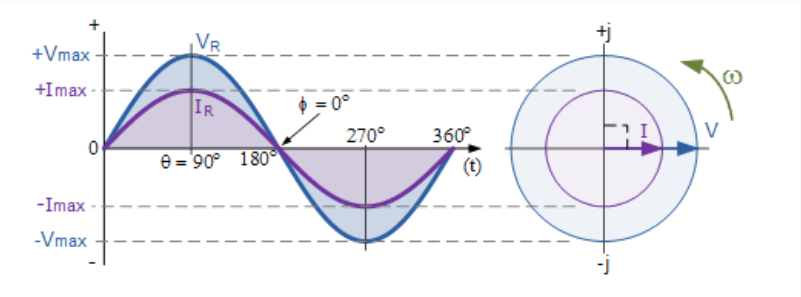

Figure 1.5 Sinusoidal wave forms of AC Resistance [Basic Electronics Tutorials].

We can see that at any point along the horizontal axis the instantaneous voltage and current are in-phase because the current and the voltage reach their maximum values at the same time, that is their phase angle θ, is 0^o. Then these instantaneous values of voltage and current can be compared to

give the ohmic value of the resistance simply by using ohm´s law. Consider the circuit in figure 1.8 consisting of an AC source and a resistor [Basic Electronics Tutorials].

The instantaneous voltage across the resistor, V_R, is equal to the supply voltage, V_t is given as:

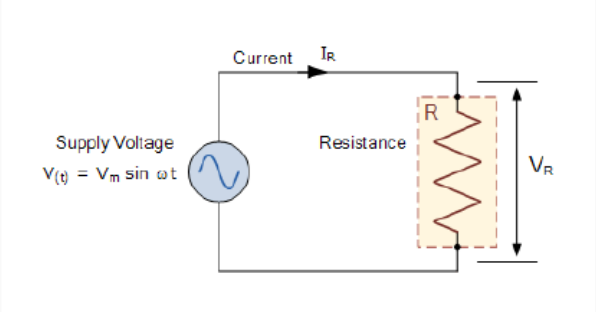

Figure 1.6 Resistor in a circuit [Basic Electronics Tutorials].

$V_R = V_{max}\sin(\omega t)$ Equation 1.7

The instantaneous current flowing in the resistor will therefore be:

$$I_R = \frac{V_R}{R} = \frac{V_{max}}{R}\sin(wt) = I_{max}\sin(wt)$$ Equation 1.8

As the voltage across a resistor is given as $V_R = I*R$, the instantaneous voltage across the resistor above is given as:

$V_R = I_{max}R\sin(\omega t)$ Equation 1.9

1.3.5.2 AC Capacitance

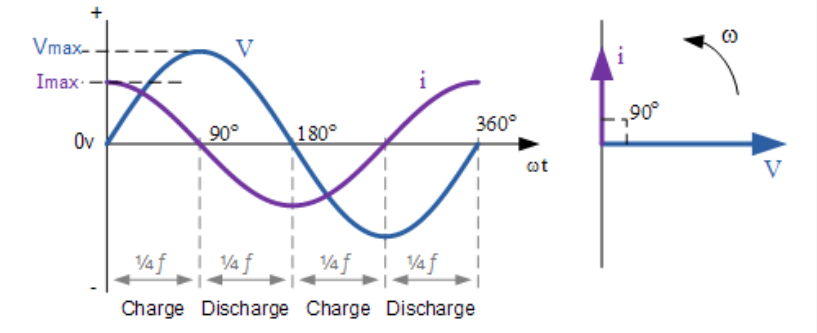

Figure 1.7 Phasor diagram- sinusoidal wave forms of AC Capacitance [Basic Electronics Tutorials].

When phase angle $\theta = 0^o$, the rate of change of the supply voltage is increasing in a positive direction resulting in a maximum charging current at that instant in time. As the applied voltage reaches

its maximum peak value at 90^o for a very brief instant in time the supply voltage is neither increasing nor decreasing so there is no current flowing through the circuit (Figure 1.8) .

As the applied voltage begins to decrease to zero at 180^o, the slope of the voltage is negative so the capacitor discharges in the negative direction. At the 180^o point along the line the rate of change of the voltage is at its maximum again so maximum current flows at that instant and so on.

Then we can say that for capacitors in AC circuits the instantaneous current is at its minimum or zero whenever the applied voltage is at its maximum and likewise the instantaneous value of the current is at its maximum when the applied voltage is zero.

From the waveform above (Figure 1.7), we can see that the current is leading the voltage by 1/4 cycle or 90^o as shown by the vector diagram. Then we can say that in a purely capacitive circuit the alternating voltage lags the current by 90^o.

Capacitors do not behave the same as resistors. Whereas resistors allow a flow of electrons through them directly proportional to the voltage drop, capacitors oppose changes in voltage by drawing or supplying current as they charge or discharge to the new voltage level. The flow of electrons “through” a capacitor is directly proportional to the rate of change of voltage across the capacitor. This opposition to voltage change is another form of reactance, but one that is precisely opposite to the kind exhibited by inductors.

Expressed mathematically, the relationship between the current “through” the capacitor and rate of voltage change across the capacitor is as such:

$$i = C\frac{dv}{dt} \qquad \text{Equation 1.10}$$

$$v = v_0\cos(\omega t) \qquad \text{Equation 1.11}$$

$$i = C v_0\sin(\omega t) \qquad \text{Equation 1.12}$$

The expression $\frac{dv}{dt}$ is one from calculus, meaning the rate of change of instantaneous voltage (v) over time, in volts per second. The capacitance (C) is in Farads, and the instantaneous current (i), is in amps [Basic Electronics Tutorials].

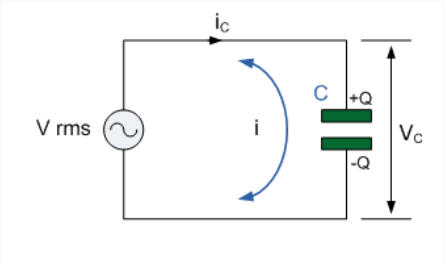

Figure 1.8 Capacitor in a circuit [Basic Electronics Tutorials].

1.3.5.3 Reactance

Reactance takes two forms: inductive (X_L) and capacities (X_C). By definition, $X_L = 2\pi fL$ and $X_c = 1/(2\pi fC)$, where f is the frequency of interest, L is inductance, and C is capacitance. $2\pi f$ can be substituted for by the angular frequency ω to represent $X_L = \omega L$ and $X_C = (\frac{1}{wc})$ [Basic Electronics Tutorials].

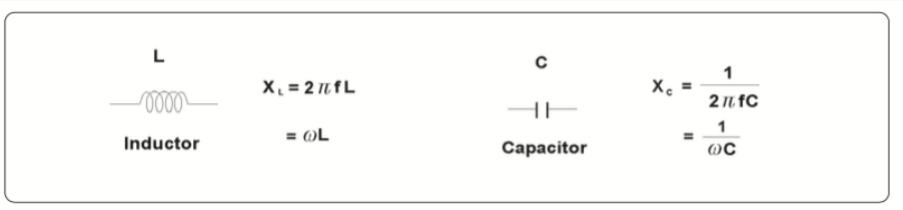

Figure 1.9 Reactance in two forms: inductive (XL) and capacitive (XC).

1.3.5.4 Capacitive reactance

Unlike a resistor where the opposition to current flow is its actual resistance, the opposition to current flow in a capacitor is called reactance. Like resistance, reactance is measured in Ohm's but is given the symbol X to distinguish it from a purely resistive R value and as the component in question is a capacitor, the reactance of a capacitor is called capacitive reactance, (X_c). Since capacitors charge and discharge in proportion to the rate of voltage change across them, the faster the voltage changes the more current will flow. Likewise, the slower the voltage changes the less current will flow. This means then that the reactance of an AC capacitor is "inversely proportional" to the frequency of the supply [Meredith Damien Gall et al., 1996].

1.3.5.5 Inductive reactance

The opposition to the current flowing through a coil in an AC circuit is determined by the AC Resistance of the coil with this AC resistance being represented by a complex number. But to distinguish a DC resistance value from an AC resistance value, which is also known as Impedance, the term reactance is used. A voltage applied to a purely inductive circuit "LEADS" the current by a quarter of a cycle or 90^0, as shown in figure 1.11 [Meredith Damien Gall et al., 1996].

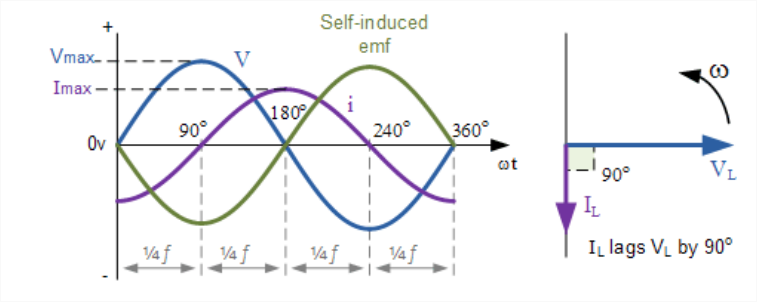

Figure 1.10 Phasor diagram- sinusoidal wave forms for AC inductance [Basic Electronics Tutorials].

Inductors do not behave the same as resistors. Whereas resistors simply oppose the flow of electrons through them (by dropping a voltage directly proportional to the current), inductors oppose changes in current through them, by dropping a voltage directly proportional to the rate of change of current. In accordance with Lenz's Law, this induced voltage is always of such a polarity as to try to maintain current at its present value. That is, if current is increasing in magnitude, the induced voltage will "push against" the electron flow; if current is decreasing, the polarity will reverse and "push with" the electron flow to oppose the decrease. This opposition to current change is called reactance, rather than resistance. Expressed mathematically, the relationship between the voltage dropped across the inductor and the rate of current change through the inductor is as such:

$$v = L\frac{di}{dt} \qquad \text{Equation 1.13}$$

$$i = I_0\cos(\omega t) \qquad \text{Equation 1.14}$$

$$v = L\,I_0\sin(\omega t) \qquad \text{Equation 1.15}$$

The inductance (L) is in henrys, and the instantaneous voltage (v) is in volts [Meredith Damien Gall et al., 1996].

1.3.5.6 Single and multi-frequency impedance measurements

Single frequency measurement uses sine or cosine waves to measure the complex impedance, responding to the single frequency input signal. Although single frequency measurement can be efficient in assessing one characteristic of the material, it is not enough when the aim of the study is the system characterization. Multi-frequency measurement uses a frequency sweep allowing us the complete characterization of the system.

1.3.5.7 Measurement in frequency and time domain

In impedance spectroscopy it is possible to represent the data in two different domains, time domain (figure1.11) and frequency domain (figure1.12).

In the time domain, signals are represented as signal, amplitude, versus time.

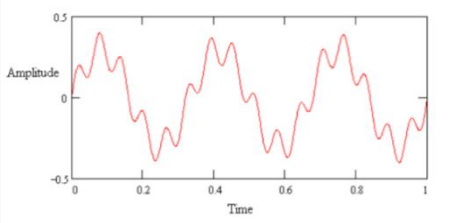

Figure 1.11 Sine waves in time domain.

In frequency domain the data is plotted as amplitude versus frequency.

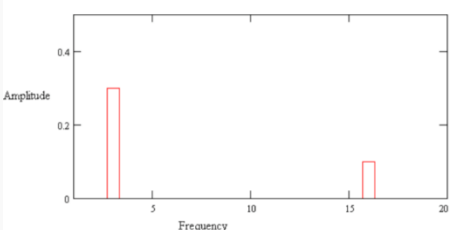

Figure 1.12 Sine waves in frequency domain.

A transform is used to switch between the domains. The Fourier transform takes time domain data and generates the equivalent frequency domain data. The inverse Fourier transforms changes frequency domain data into time domain data.

1.3.5.8 Data representation

Besides many variations in presenting a spectrum of passive electrical properties, the most popular form is the magnitude, phase angle, real or imaginary part versus frequency. Bode-plot offer a way of presenting phase and magnitude information from a rotating vector. This form of presentation is particularly useful for measurements performed over a wide range of frequencies, which often result in a large amount of information being cramped into a small section of a phasor diagram [Resistors and Capacitors in Parallel]. This consists of two subplots, the Bode magnitude plot and the Bode phase plot respectively. A Bode magnitude plot is a graph of log magnitude against log frequency. A Bode phase plot is a graph of phase against log frequency, which usually used in conjunction with the magnitude plot [Liu, 2006]. Unlike the Nyquist plot the bode plot show frequency information.

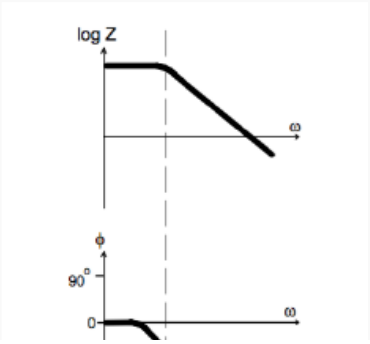

Figure 1.13 Bode plot.

Nyquist-plot is a complex plane, which plots the negative of the imaginary part of impedance against the real part of impedance. Notice that, in this plot the y-axis is negative and that each point on the Nyquist plot is the impedance at one frequency. Low frequency data are on the right side of the plot and higher frequencies are on the left. Figure 1.14 gives an example of the Nyquist Plane. The disadvantage of this data presentation is that it cannot directly indicate frequency response [Liu, 2006]. On the Nyquist plot the impedance can be represented as a vector (arrow) of length |Z|.

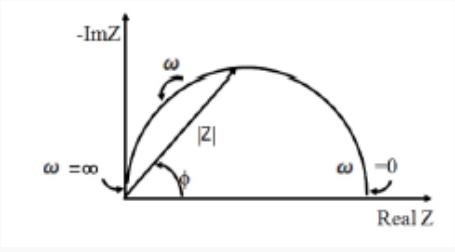

Figure 1.14 Nyquist plot.

1.4 Bio impedance

1.4.1 Historical introduction

The first reported contact with the electrical properties of biological tissue was done by Luigi Galvani who, on 1780, showed that the living body utilizes electricity to control muscle movement and that nerves act as electrical wires. After several developments in electronic instrumentation as the Volta electrochemical battery, the continuous DC current source developed by Volta in 1800, the galvanometer in 1820, the high AC voltage/current pulse generators in 1831 and the continuous AC current sources from 1867, the detection of small bio electrical currents became possible. The term ‘impedance’ was coined by Heaviside, around 1880. About the same time, measurement of electrical

conductance in human skin began and became the precursor of the lie detector. From then on, many clinical applications based upon bio impedance have been developed, including measuring cardiac minute volume non invasive, measuring lung respiration activity, and taking electronic biopsies for diagnosis of skin cancer.

1.4.2 Bio impedance measurements

Spectroscopy is the analytical study of electromagnetic spectra, including the visible spectrum, ultraviolet and infrared radiation, and all other portions of the electromagnetic spectrum as well. Dielectric properties of materials are important in determining how electromagnetic energy interacts, with materials, the study of their dependence on wavelength on frequency is termed bio impedance spectroscopy [Nelson and Trabelsi, 2008]. Electrical impedance measurements are an important tool for food material characterization. The cells of meat and vegetables are surrounded by an insulating membrane, the cytosol and the extra cellular fluids are electrolytes. The electrolytes behave like ohmic resistors up to hundreds of MHz On the other hand, membranes form capacitive elements due to their high resistance. As a result of the different mineral substances and organic acids present, along with other components that are susceptible to dissociation, the high electrolytic conductivity of fruits and vegetables is distinguished [Pliquett, 2010].

1.4.3 Electrical impedance spectroscopy

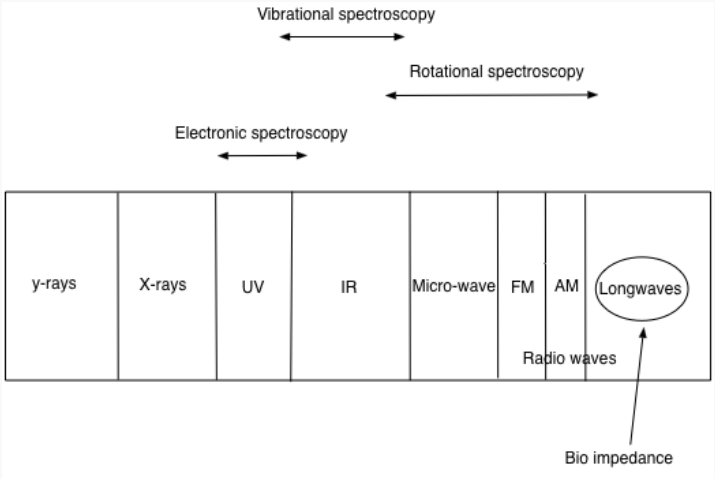

Figure 1.15 Electromagnetic spectrum.

Biological tissues have a complex impedance profile which changes with respect to frequency. This is caused by dispersion mechanisms which govern how electromagnetic field interacts with the tissue at the cellular and molecular level [O'Toole et al., 2015]. Any matter can be characterized

electrically, either by active electrical properties, current and voltage sources, or by passive electrical properties. Passive means that the object has no electric sources but is composed of dissipate elements like ohmic resistors and conservative elements like capacitances and inductances. Bio impedance denotes the passive electrical properties of the biological material. The impedance characterizes how an object impedes the current flow due to an outer electric field. The electrical impedance spectrum, in low frequency range, of biological tissues depends on the state of cellular structure. The current I, as it passes across a section of a material of impedance Z, drops the voltage V, established between two given points of the same section, Ohm's law: $V = IZ$, where V and I are complex scalars and Z is the complex impedance. The result of the rlrctrical impedance spectroscopy EIS, measurements is a set of complex (magnitude and phase) of impedance versus frequency. EIS analyses the subsequent electrical response of a subject when small AC signals are applied and characterizes the physic-chemical properties of the system [Pliquett, 2010].

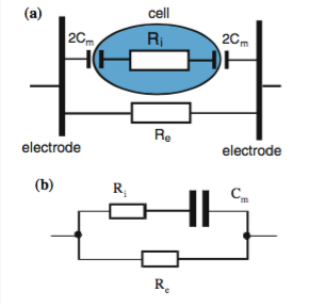

Figure 1.16 (a) Capacitive and resistive elements in a simplified cell. (b) Circuit for the β-dispersion. Cm the membrane capacitance, Ri the intra cellular resistance, and Re the resistance of the extra cellular electrolytes (Pliquett,2010)

1.4.4 Frequency dispersion

The permittivity (measure of how an electric field affects, and is affected by, a dielectric medium of biological tissue) exhibits distinct frequency dispersion. At low frequencies (100 mHz-100 Hz), the lateral movement of ions along insulating membranes causes the *α*-dispersion. The polarization of cell membranes, blocking the flow of ions between the intra and extra cellular media [O'Toole et al., 2015] yields the *β*-dispersion between 1 kHz and 10 MHz depending on the size of the cells and the conductivity of the surrounding electrolytes. In a frequency range up to GHz, macro-molecules mostly give rise to the *γ*-dispersion the *δ*-dispersion is caused by water and ranges from 2 GHz up to 25 GHz and is often not distinguished from *γ*-dispersion [Pliquett, 2010] It follows that changes occurring in a biological test sample at the cellular or molecular level should be reflected in the impedance spectra of that sample. In this study we will work with *β*-dispersion, which affect the cell membrane. From this, we may assume that the impedance values is indicative of the average integrity of cell membranes, or the volume fraction within the sample of cells surrounded by cell membranes [O'Toole et al., 2015].

1.4.5 Measurement principles

Direct and indirect measurements can be employed in food. While direct measurements access the electric properties of the material under test (MUT), indirect measurements correlate the characteristics of the MUT with secondary quantities, medium conductivity, influenced by the metabolites of living cells, and others [Pliquett, 2010].

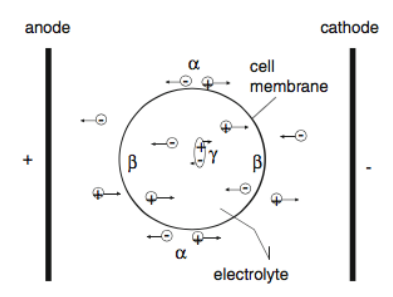

Figure 1.17 Polarization mechanisms at cell situated between two electrodes [Pliquett, 2010].

1.4.6 Sensitive and selectivity

The practical suitability of a measuring method is determined by its sensitivity and selectivity. In bio impedance there are a lot of external factors influencing the electrical properties of the MUT. Among the factors that are involved in the dielectric properties values, the nature of the material that implies the composition and structure is the most common. Some other factors, such as frequency and temperature, are involved with the maturity stage of the agricultural product. Ionic components have significant effects on the dielectric properties. Another factor is the density, because the amount of mass per unit of the volume (density) has a definitive effect on the interaction of the electromagnetic field and the involved mass. Thus, it is important to careful select the qualities we want to measure with impedance. The monitored quality should influence the electrical properties overwhelmingly and other factors should not compromise the selectivity [Pliquett, 2010]. For instance, extending the bandwidth of the measurement combined with physically relevant models, can help relate the shape of the spectra with the actual mechanisms and changes at the cellular level, but invariably the successful approach is choosing applications where the properties of interest influence the electrical spectra response on the sample [O'Toole et al., 2015].

1.4.7 Electrical models

The use of electrical models are the most common method to analyze the bio impedance spectra. In this method the measured spectrum is fitted onto an equivalent electrical circuit and the

information of spectrum is summarized in different descriptive features based on similarities between the electrical circuits and the biological tissues. These models have been basically introduced and applied as explanatory features of bio impedance measurements and have been known to have limitations [Nejadgholi et al., 2015]. In EIS, is measured an electrochemical cell complex impedance over a wide range of AC frequencies. Typically, several cell elements and cell characteristics contribute to the systems EIS spectrum. A partial list of possible elements includes:

- Electrode Double
- Layer Capacitance
- Electrode Kinetics
- Diffusion Layer
- Solution Resistance

Unfortunately, the system's impedance at any given frequency usually depends on more than one cell element. This greatly complicates the analysis of EIS spectra. The most common method used to analyze EIS spectra is equivalent circuit modeling. Is simulated the cell incorporating the elements. The behavior of each element is then described in terms of "classical" electrical components (resistors, capacitors, inductors) plus a few specialized electrochemical elements (such as Warbug diffusion elements). The arrangement of the elements into logical series and parallel combinations is critical to the success of the modeling effort. Each element in the model has a known impedance behavior. The impedance of the element depends on the element type and the value(s) of the parameter(s) that characterize that element. For example, the impedance of a capacitor excited by a sine wave at frequency f is described by the Equation 1.16.

$$Z_c = \frac{1}{j^2 \pi f C}$$ Equation 1.16

Zc is the complex impedance, j is $\sqrt{-1}$, f is the frequency in Hertz and C is the capacitor's value in Farads. In order to study the electrical properties of fruits, the cell structure has been simulated by equivalent electrical circuits. The values of circuit components determine the electrical response. A single cell isolated from a tissue can be simulated by an equivalent circuit consisting of resistors and capacitors arranged in series and parallel. Thus, a tissue block can be presumed to be a network of cells, which contain numerous arrays of mini-circuits [Liu, 2006].

1.4.7.1 Cole model

The Cole model simplified biological tissue into a two-branch parallel circuit. Two resistors represent the extra cellular space resistance, and intra cellular space resistance, a capacitor represents the cell membrane capacitance.

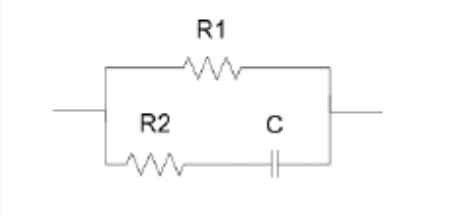

Figure 1.18 Cole Model R1 is the extra cellular space resistance, R2 is the intra cellular space resistance, C is the cell membrane capacitance [Liu, 2006].

1.4.7.2 Hayden Model

Hayden analyzed the cells of potato and observed that, according to plant cell structure, the cells are equivalent to many small capacitors and resistors connected in parallel with their cell walls.

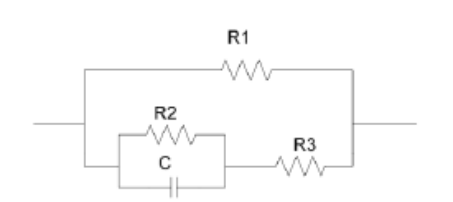

Figure 1.19 Hayden Model R1 represents the resistance of all cell walls, R2 represents the resistance of all membranes of all actual cells, R3 represents the resistance of cytoplasm of actual cells, and C represents the capacitance of all membranes of actual cells.

1.4.7.3 Double-shell Model

This model includes the cell wall resistance (R1), cytoplasm resistance (R2), vacuole resistance (R3), plasma membrane capacitance (C1), and tonoplast capacitance (C2).

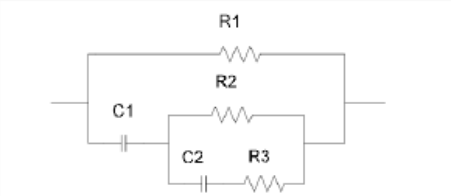

Figure 1.20 Double -shell model [Liu, 2006].

1.5 Impedance spectra and data analysis

Bio impedance spectroscopy is a non-invasive and low cost method to measure electrical responses of living tissues applying an alternating current at a range of frequencies. Single frequency and multi-frequency bio impedance have been measured and modeled in many research applications to explain how different sources of variations affect the response of a living tissue. However, classification of measured bio impedance spectra in order to classify the fruit is a particular challenge. The signal is recorded on the surface of the fruit and reflects the internal phenomena on the fruit.

There is a vast amount of statistical methods to analyze impedance data. Because impedance measurements are done as frequency sweeps, producing large amounts of correlated and possible redundant data, the implications for inferential statistics are discussed together with data reduction solutions.

Often in bio impedance measurements, we want to analyze more than one variable per sample or measurements. In order to maximize the changes of finding the most important effects in bio impedance, we may acquire the impedance at multiple frequencies from one measurement. A common method is to assume that the electrical properties of the sample can be described by an electrical equivalent model, such as Cole model, and to estimate the component values by fitting the measurement to the mathematical expression of the model. With a good agreement between the model and the measurement, this approach reduces the measurements into a few uncorrelated parameters which are easier to handle statistically. Data reduction can also be done with the principal component analysis, PCA. PCA maps the whole data on its salient part of information on first eigenvectors as features.

1.5.1 Data pre prossessing

The data from highly sensitive instruments can be influenced by subtle changes in settings or conditions and hence are often contaminated by noise, or more precisely, non-discriminatory sample-specific signal ranging from broadband back-ground [Randolph, 2006]. Pre-treatment of raw spectral data is critical for generating reliable, interpreted models using multivariate analysis techniques.

Table 1.1 Listing of used data scaling methods in bio impedance multivariate analyses.

Method	Equation	Goal
Scaling	$x_{ik} = \frac{x_{ik}}{x_i}$	If each spectrum contains a different amount of variance, large intensities are magnified more than low intensities. dividing each spectrum by its total energy produces a set of unit-length vectors.
UV	$x_{ik} = \frac{\frac{x_{ik}}{x_i}}{s_k}$	All variables are equally important.
Pareto	$x_{ik} = \frac{\frac{x_{ik}}{x_i}}{\sqrt{s_k}}$	Reduce the influence of intense peaks while emphazing weaker peaks that may have more biological relevance.

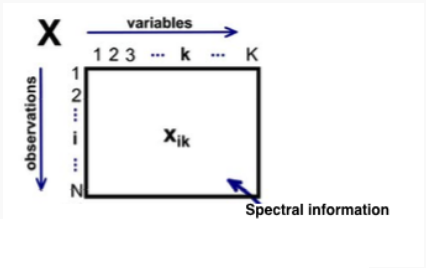

Figure 1.21 Data matrix.

1.5.2 Multivariate analysis

Principal component analysis (PCA) is one of the most commonly used multivariate analysis methods. It provides unsupervised pattern recognition, reduced dimensionality, and easy visualization of the data [Luthria et al., 2011]. Principal component analysis assumes that there is a linear orthogonal basis for representation of a given data space and uses decorrelation techniques to find the basis. In the context of this work, let N denote the number of frequencies in which the bio impedance is measured and M the number of taken bio impedance measurements. Having formed the *M*N* data matrix, X, we assume that the number of uncorrelated data variables, r, where $r = Rank(X)$, is less than the number of frequencies, N. PCA forms the covariance matrix of the mean centered data matrix, $X - mean(X)$, which includes covariance between frequencies. This covariance matrix $C_x = [C_{ij}]$ can be written as

$$C_{ij} = \sum_{K-1}^{M} X_{ki} X_{kj}, i, j = 1,2,..,N \qquad \text{Equation 1.17}$$

Where X_{ij} is representing the element of mean-centered data matrix corresponding to measured impedance in *ith* observation and *jth* frequency. Full rank principal component expansion of X is given as in the following equation

$$C_{ij} = \sum_{i=1}^{N} \sigma_i^2 v_i^T v_i \qquad \text{Equation 1.18}$$

in which $\sigma_i = \sigma_1 \geq \sigma_2 \geq \sigma_3 \geq \ldots \sigma_N > 0$ are singular values of $X - mean(X)$, and $v_i = [v_{1i}, v_{2\ldots} v_{Mi}]^T$ with $i = 1, 2, \ldots, N$ are right singular vectors of $X - mean(X)$. These eigenvectors form an orthogonal basis for impedance data representation in frequency domain. For dataset, eigenvectors [v_1, $i = 1, \ldots, r$] are calculated and each spectrum is mapped on these eigenvectors [Isar Nejadgholiet al., 2015]. The scores obtained from this mapping are considered as PCA scores of that spectrum. The scores produced from PCA are observation rows of X projected onto a hyperplane within the data that describes the covariance of X, or the covariance between X and the response matrix, respectively. Loadings from PCA are the directions of the hyperplane mentioned above with respect to the original X variables, and function as good "summaris" of the variables influence on the model [Worley et al., 2013]. For a new spectrum which was not present in data matrix, X, principal components are obtained by mapping the new spectrum on v_i. The PCA is a way of feature extraction and not a complete classification method, to perform classification these features should be analyzed by a classifier [Nejadgholi and Bolic, 2015].

Partial least squares regression (PLS) is a supervised classification technique. The scientist can select sample characteristics representative of some classes and write an algorithm to use these references for the samples classification. In these study the PLS was used to build a linear calibration model to predict Brix^o of grapes [Eriksson, L., et al,. 1999].

1.5.3 Analysis of variance

ANOVA can be used to statistically compare more than two groups of measurements. For example, three different fruits, bananas, kiwis and pears. This test compares the variance within each group to the variance between the groups. The one-way ANOVA is useful when we study only one factor which groups the measurements, for example type of fruit. If we want to study how frequency in addition to tissue type affects the bio impedance, we have a factorial design with two factors and may use the two-way ANOVA. The output of this test gives us the statistics, F-statistic and p-value, which tell us whether each of the two factors have a significant effect on the impedance value. In addition, the two-way ANOVA can test whether there is a significant interaction between the two factors, the difference in bio impedance among fruits may depend on the frequency [Tronstad and Pripp, 2014].

1.6 Literature review

1.6.1 Impedance analysis on plant tissue

Fruits are biological objects with a complex structure of several tissues consisting of the three-dimensional arrangement of cells. All the fruits are different with their own composition and food values. Fruit ripening is a process where the matured raw fruits undergo through several physiological changes over a certain time period. Fruits are essentially required to be properly ripened to ensure the development of all the nutrients. As the proper ripening of fruits conforms the maximum nutritional potential of the fruit, the under ripening and the over ripening are not desirable. Therefore, the ripening process of the fruits is important to be studied in order to eat the fruits when the best nutrients are available [Chowdhury et al., 2015] During the last decades, various equipment for impedance measurements appear in the market. Although constructed for other purpose, network analyzers have been the most used in bio impedance measurements [Pliquett, 2010]. Electric impedance consists in passing alternating current of different frequencies across fruit and vegetable tissues. Impedance describes the passive electrical behavior of any material in terms of its capacity to dissipate and to conserve electrical charge. EIS can provide a method of simultaneously examining changes occurring in fruit tissue during ripening, since it can be used to detect changes in the resistance of intra cellular and extra cellular compartments. This section provides a review on impedance measurements on plants.

1.6.2 Impedance analysis on apples - acid measurements

EIS has been used extensively to characterize electrical properties of plant tissue. Some researches explores the potential connections between electrical impedance and the major parameters can contribute to fruit taste. Experiments were performed by Castro Giraldez (2010) and Fang (2007) in order to find relations with apple physiological compounds and dielectric properties. To determine the state of fruit maturity through the potential use of dielectric spectroscopy, a study was conducted to find relations with apple physiological compounds, such as sugar content and malic acid. A non-destructive control method was presented for the prediction of climacteric fruits maturity. Measurements were taken at frequency ranging from 500 MHz to 20 GHz. A new good correlation was found between apples Thiault Index and a new defined Dielectric Maturity Index, which is related to the loss factor at two punctual frequencies [Fang et al., 2007]. Experiments were performed on four apple varieties, Granny Smith, Fuji, Pink Lady and Red Delicious. Electric impedance was measured using a Impedance/Gain-phase Analyzer at frequency range from 1 Hz to 1 MHz. Soluble solid content (SSC), titrable acidity (TA) and pH value of apple were measured as chemical parameters. It was found that the four apple species cannot be classified on the basis of their soluble solid content. However, the four apple species can be divided into three groups according to the ratio of Brix^{o} to TA, namely the low-acid variety, the high-acid variety, and the medium-acid variety. At the frequency range of 500 MHz to 20 GHz, another dielectric

measurement was applied to apples with different sugar contents during ripening [Fang et al., 2007] The objective of the study was to determine the optimal time for eating apple. Various good correlations between the maturity index and the Thiault index were found. Prospective data of some chemical components of apples were presented in the study [Fang et al., 2007]. These investigations reveal that the EI approach offers a new method for apple quality assessment.

1.6.3 Impedance analysis on kiwifruit

The electrical impedance of kiwifruit was studied by Bauchot (2000) during fruit ripening. Measurements were made on whole fruit. Alternating current at frequencies between 50 Hz and 1 MHz was passed through fruit and tissue samples. During ripening it was observed a small change in impedance values, despite a decrease in firmness. This was unexpected since studies with other fruits have shown considerable reduction in impedance during ripening. It was suggested that the mobility of electrolytes inside the cell wall did not change during ripening through electrolyte leakage analysis. The authors concluded that the selectivity of the impedance method was not sufficient for practical use. The physicochemical interactions taking place within the cell wall have a major impact on the tissue impedance.

1.6.4 Impedance analysis on bananas, mango and garut citrus - ripeness measurement

The characterization of fruits has been an important issue in the automatic sorting of fruits. Fruit-ripeness determination research is increasingly gaining prominence in the food industry [Alfatniet al., 2013)]. The quality of the fruits, at the time of consumption depends on the maturity stage. These changes should, in principle, be reflected in the shape of β-dispersion, making the spectra potentially useful indicator of the state and progress of these properties. EIS studies have been conducted as a non-destructive investigation evaluation method to study the electrical impedance variations in banana [Chowdhury et al., 2015; Soltani et al., 2010], mango ripening [Rehman et al.,2011; Alfatni et al., 2013] and garut citrus fruit [Jajang et al.,2012]. Effective resistance and effective capacitance vs. frequency have been determined. The impedance spectrometric technique has been developed and applied successfully in the characterization of raw and ripe mangoes at 1KHz. Data from this study clearly shows that effective resistance of the fruit under test increases with time and reaches a peak and starts decreasing with the passage of time. Initially when fruit was clearly raw and had green color, effective resistance was lowest and effective capacitance was highest. When fruit started changing color, effective resistance started increasing and effective capacitance started decreasing and reached a highest value and lowest, on the same day [Rehman et al., 2011.]. EIS studies conducted on banana shows that impedance, phase angle, real and imaginary part of the banana varies with the frequency as well as with the ripening state. Chowdhury (2015) observed that the banana impedance increases during

ripening. Soltani (2010) reported the EIS was capable of classifying the banana fruits during ripening period and of assessing changes based on the quality parameters, as the linear regression frequency value of 1MHz offers a satisfactory correlation for both SSC and firmness with relative permittivity, which was selected for the development of the sensing system. Juansah (2012) investigated the physicochemical properties associated with ripening in garut citrus fruit. The aim of this study was to relate specific quantitative metrics to the behavior of electrical properties and modeling of citrus fruits including internal resistance and its capacitance changes using nondestructive test. The acidity and firmness changes lead to changes in internal electrical properties. Based on the new model, membrane capacitance and tissue resistance also can describe the acidity and firmness phenomenon of fruits. The resistances of part component of circuit model were declined as pH increases. While, both of capacitance and pH have positive correlations. In the firmness phenomenon, both of firmness and resistance have a line change, where increasing firmness, it also increases the value of resistance. But it not happens in capacitance behavior as firmness change. The capacitance decreased as firmness improved. Thus far, the link between impedance spectra and the state of ripeness of maturity is only indicated rather than definitive. More robust correlations are required before bio impedance spectra can be used as a metric ripeness or maturation [O'Toole et al., 2015].

1.6.5 Impedance analysis on grapes, apple and persimmon - tissue damage

Internal fruit damage is one of the most critical problems affecting the quality of agricultural products. The identification of defects or damage in produce has been highlighted as a useful application—particularly when the damage or defect cannot easily be detected by visible inspection [O'Toole et al., 2015]. Numerous applications for capacitance and inductance probing sensors in agriculture quality estimation have been used by numerous researchers worldwide. Electrical impedance spectroscopy has the capability to detect several tissue damage in fruit. Thus, EIS may also provide a technique that can detect damage that has occurred within fruit flesh as a result of physical injury and/ or development of physiological disorders. Harker and Forbes (1997) explored mechanisms of chilling injury by observing the change in impedance spectra subject to different storage conditions. It was found that chilling injury during storage of New Zealand-grown ‘Fuyu’ persimmon fruit was indicated by changes in the cytoplasmic resistance at low frequencies. The effect of apple- bruising on the impedance spectra has been investigated. The advantage of using impedance spectroscopy over traditional methods is that the result is immediate and non-destructive. Jackson and Harker (2000) found that changes in resistance that occurred as a result of fruit impact was the best predictor of bruise weight. Impedance ratios were not shown to be effective except where bruising was heavier. Ideally, for the impedance ratio to be effective, the higher frequency should be sufficiently high to independent of changes in cellular structure. Berry cell compartment is apparently lost during ripening. Caravia, et al. (2015) studied the correlation between electrical impedance of shiraz berries and cell vitality during

ripening. It was found that berries with cellular damage caused by microwaving, or freezing and thawing, decrease the impedance dramatically. This decrease indicates that there are physical or chemical changes in berry cells and/or walls that correlate with loss of vitality as measured using the FDA vital stain.

1.7 Development and ripening in fruit

Post-harvest physiology is the scientific study of the physiology of living plant tissues after have been denied further nutrition by picking. It has direct applications to post harvest handling in establishing the storage and transport conditions that best prolong shelf life. Is very important the post-harvest handling for the industry and scientific studies, the discovery that ripening of fruit can be delayed, and thus their storage prolonged and controlled, by preventing fruit tissue respiration. This insight allowed scientists contribute with their knowledge of the fundamental principles and mechanisms of respiration, leading to post-harvest storage techniques such as cold storage, gaseous storage, and waxy skin coatings. Another important knowledge was finding that ripening may be brought on by treatment with ethylene and thus is possible to artificially ripe the fruit, which allow to use fruit in different studies. When the fruit have a non–climacteric development is more difficult to use as a sample in laboratory studies, because after harvest the fruit development stops, so all the experiments need to be done in a small period after picking [El-Ramady et al., 2015].

Development and ripening in fruit is a unique phase in the life cycle of higher plants which encompasses several stages progressively such as fruit development, its maturation, ripening and finally senescence. During ripening phase, several physiological and biochemical changes take place through differential expression of various genes that are developmentally regulated. Mostly fleshy fruit ripen in the presence of ethylene and once ripening has been initiated proceeds uncontrollably. Ethylene involves several responses during ripening through a signaling cascade on thousands of genes participate which not only sets in ripening but also responsible for its spoilage. The spoilage includes excessive softening and changes in taste, aroma and skin color. This unavoidable process brings significant losses to both farmers and consumers alike [Bapat et al., 2010] Fruit have changes, although variable among species, generally include modification of cell wall structure, and texture, conversion of starch to sugars, increased susceptibility to post-harvest pathogens, alterations in pigment biosynthesis and accumulation, and heightened levels of flavor and aromatic volatile [Giovannoni, 2001].

Gaseous plant hormone ethylene has been assigned a major role in the ripening of climacteric fruits. Considerable evidences at the physiological, biochemical, and molecular levels have been accumulated which indicated ethylene mediated regulation of ripening at various levels. This includes ethylene biosynthesis its perception by the target cells through receptors, signal transduction cascade involving both positive and negative regulators and finally regulation of target gene expression by transcription factors such as ethylene response factors [Bapat et al., 2010].

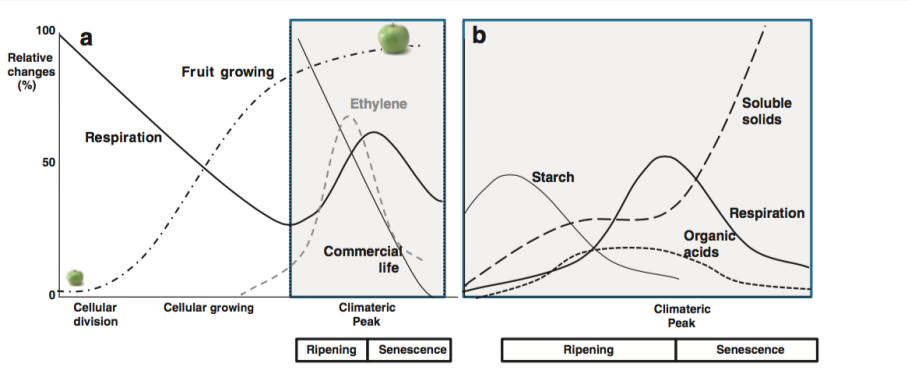

Figure 1.22 a)Qualitative evolution of respiration rate, fruit growing, ethylene levels and commercial life of climacteric fruit; b)Qualitative evolution of starch, soluble solids and organic acids content during the ripening and senescence [Castro-Giráldez et al., 2010].

Although most fruit display modifications in color, texture, flavor, and pathogen susceptibility during maturation, two major classifications of ripening fruit, climacteric and non-climacteric, have been utilized to distinguish fruit on the basis of respiration and ethylene biosynthesis rates. Climacteric fruit, such as tomato, avocado, banana, peaches, plums and apples, are distinguished from non-climacteric fruits, such as strawberry, grape and citrus, by their increased respiration an ethylene biosynthesis rates during ripening. Although non-climacteric fruits may respond to ethylene, ethylene is not required for fruit ripening from species in this classification. In contrast, ethylene is necessary for the coordination and completion of ripening [Giovannoni, 2001]. There are two distinct ethylene biosynthesis systems. System 1 corresponds to low ethylene production in the pre-climacteric period of climacteric fruit and is present throughout the development and ripening of non-climacteric fruit. System 2 refers to an auto-stimulated massive ethylene production, called ‘auto catalytic synthesis’ and is specific to climacteric fruit. Therefore, the major differences related to ethylene between climacteric and non-climacteric fruit are the presence or absence of auto catalytic ethylene production. However, external application of ethylene during ripening to non- climacteric fruit may hasten the process in some cases [Bapat et al., 2010].

1.7.1 Climacteric fruits

Apple (Malus spp.)

Apple is one of the most important fruit crops worldwide. There are more than 7500 known cultivars of apples. Different cultivars are available for temperate and subtropical climates. Desired qualities in commercial apple include colorful skin, absence of rusting, prolonged storage ability, high yields, disease resistance [Bapat et al., 2010] Apple is a common fruit variety with moisture content

more than 80% of the fruit weight. Cells are the functional units of apple tissue, and their state determines manly the biochemical transformation of apple during maturation process. The edible part of it is a rich source of fiber and antioxidants. Taste, aroma and freshness are ranked as the top three criteria from consumer's perceptions as the factors which attract consumers to purchase fruit [Fang et al., 2007; Liu, 2006].

Apple is a climacteric fruit and is characterized by the starch accumulation during fruit growth, which is hydrolyzed to monosaccharides, mainly glucose and fructose, during the ripening process. Starch hydrolysis is a process that requires high energy consumption and it is related to an increase of fruit respiration rate (climacteric crisis), until reaching its maximum at the end of ripening (climacteric peak). The main biochemical changes of fruit maturity are produced during the climacteric rises. A climacteric rise in ethylene production precedes the increase in respiration rate, suggesting that ethylene is the hormone that triggers the ripening process. Organic acids are also strongly related to maturity process of climacteric fruits. The relationship between soluble solids content and organic acid concentration is called Maturity Index and is usually used in industry as a reference parameter of fruit state. Thiault Index (TI) is one of the maturity indexes frequently employed in apple fruit. Currently, the industry uses destructive methods to ensure the quality standards demanded by consumers. In this context, impedance spectroscopy is presented as an interesting technique to monitor, fruit quality standards and ripening changes [Castro-Giráldez et al., 2010].

Banana (*Musa spp.*)

Bananas constitute a major staple food crop for millions of people in developing countries. Banana is a typical climacteric fruit with a very short post-harvest life. Many varieties of banana fruits are ripened artificially by exposing them to hydro- carbons. The current methods of post-harvest management which include cold storage, chemical spray, chemical coating or gamma irradiation of fruits are not sufficient to control the exaggerated ripening of banana [Bapat et al., 2010] For bananas, the relationship between the sugar content and the peel color changes is parallel. Firmness is a very good indicator in determining the quality of products, and it has been used to measure maturity and ripeness of fruit. Usually, a penetrometer is used to measure firmness of fruits and it is a destructive method. Peel color is considered as a good indicator of banana ripeness as the chlorophyll content in the peel reduces with banana ripening. The first observable sign of ripening is a color change from green to yellow. There are seven stages of banana color guide during ripening and retailers usually sell banana fruits when they are at stage four (Figure 2.3). Nevertheless, this method is based on human visual determination that can be imprecise and insufficient to assess the internal quality changes [Jamaludin et al., 2014].

Pear "Rocha" (*Pyrus spp.)*

The pattern of softening and ripening of 'Rocha' pear closely follows the climacteric ethylene rise. Pears continue to ripen after harvest. Assessment of 'Rocha' pear ripening is of major concern in

both pre and postharvest long-term storage periods. The quality for eating depends on the degree of ripeness. Currently, this depends on the destructive determination of fruit firmness through pressure tests using a penetrometer on the fruit surface. If the degree of ripeness could be determined non-destructively, it would be a useful indicator for distributors to determine when to ship the pears and for consumers to know the optimum timing for eating [Cavaco et al., 2009].

Kiwi (*Actinidia deliciosa*)

The world production of kiwi fruit was estimated at 1.3 million tons in 2008. The quality of kiwi fruit is greatly influenced by the stage of maturity. Kiwi fruit has high levels of vitamin C and citric acid. Consumer satisfaction is achieved when ripe fruit reaches at least 12.5% with low acidity SSC (at consumption). Prediction of ripe kiwifruit quality can be done by measuring total solids at harvest destructively and non-destructively (near infrared).

Tomato (*Lycopersicon esculentum*)

Tomato is a climacteric fruit. Such as other climacteric fruits, tomato have a large burst of respiration known as the climacteric rise at the onset of ripening, in concert with an autocatalytic increase in the production of ethylene. Tomato ripening is also associated to carotenoid biosynthesis.

Tomato texture is an important driver of consumer preferences for fruits. Texture not only affects consumer preference, but also has a significant impact on shelf life and transportability. Texture reflects many factors, including cell wall structure, cuticle properties, cellular turgor and fruit morphology. The tomato fruit cell wall changes during ripening, initial models suggested that one or two enzymes, such as polygalacturonase (PG), which can hydrolyze the pectin backbone of HG polymers de-esterified by pectin methyl esterase (PME) might play the major role in controlling texture changes in tomato because of the substantial changes in the levels of activity of these enzymes during the ripening process. In addition to the structural matrices of the cell wall, another important contributor to texture and fruit firmness is cellular turgor. This in turn is governed by water status within fruit and the relative distribution of water within the cell (the symplast) and the cell wall (the apoplast) [Seymour et al., 2013].

The parameters that define tomato quality are internal aspects, are not noticeable for consumers. In this context, improved methods for rapidly sensing, would be helpful in the harvest, sorting and packing operations; electrical measurements is a simple innocuous tool for material characterization, which should make the determination of electrical properties a highly effective method to enhance the quality of fruits and vegetables.

1.7.2 Non-climacteric fruits

Grape (*Vitis spp.*)

Grape is the non-climacteric fruit that grows on the woody vines. Grape exhibits a biphasic pattern of growth, the first growth phase (stage I) is separated from the second growth phase (stage III) by a period of relatively little growth (stage II). The transition from stage II to Stage III is known as “veraison”, and it includes the start of berry softening, sugar accumulation, and color development in pigmented varieties. The green stage (I) extends from the setting of the berries up to the beginning of the ripening. During this stage the main change is a rapid increase in berry size. The level of sugars remains almost constant, the acidity is high and the berries are hard, glucose is present in larger amounts than fructose, and malic and tartaric acid increase to their maximum level. The ripening stage extends from the beginning of ripening until the grapes are ripe. At this time the green color of the white varieties begins to fade and the white or yellow come into view. In red and black varieties, the development of color begins. The berries, which up to this time have remained hard, begin to soften. The metabolism of the berry changes drastically and the fruits changes from acid accumulative organ to a sugar accumulative organ. The changes in sweetness, acidity, and other constituents go forward much more rapidly. Berries enlarge rapidly during ripening. As ripeness is approached, these various changes decelerate. The ripe stage is the condition that results when the changes in the several components of the fruit have produced to a point where their combined effect on the quality to the given variety is the nearest possible approach to an ideal for a given propose. Grape has been classified as non-climacteric but studies have shown that grape berry tissues have a fully functional pathway for ethylene synthesis and that this pathway is activated just before veraison. However, the signals leading to berry expansion and softening are yet not fully understood. Several studies have been carried out to investigate the role of cell wall degradation related to enzymes and the expression of respective genes during softening of the grape berries [Bapat et al., 2010].

2 Materials and methods

2.1 Electrical impedance spectroscopy- integrate Circuit AD5933

The AD5933 is a high precision impedance converter system (Figure 2.1), from 1 kΩ to 5 MΩ, that combines three different blocks: a transmit stage, a receive stage, and a Discrete Fourier Transform (DFT) engine. The DDS (1) (Direct Digital Synthesis) core and the high speed DAC (1) generate a sine wave signal used to excite the impedance, the output programmable gain amplifier (2) (PGA) is used for conditioning the output signal – Transmit stage. The Trans-impedance amplifier (3) (TIA) converts the current that crosses the impedance into voltage.

The input PGA (4) amplifies the TIA signal. The ADC (5) (Analog to digital Converter) transform the digital signal into a sinusoidal signal. The frequency generator allows an external complex impedance to be excited with a known frequency. The response signal from the impedance is sampled by the on-board ADC – Receive stage. The DFT engine processes the data and generates real (R) and imaginary (I) number components for each output frequency which is stored in two 16 bits register – DFT engine. The output signal can be stepped in frequency from the operator's control, giving a start frequency, the frequency increment and the number of increments [AD5933 datasheet and product info 1 MSPS].

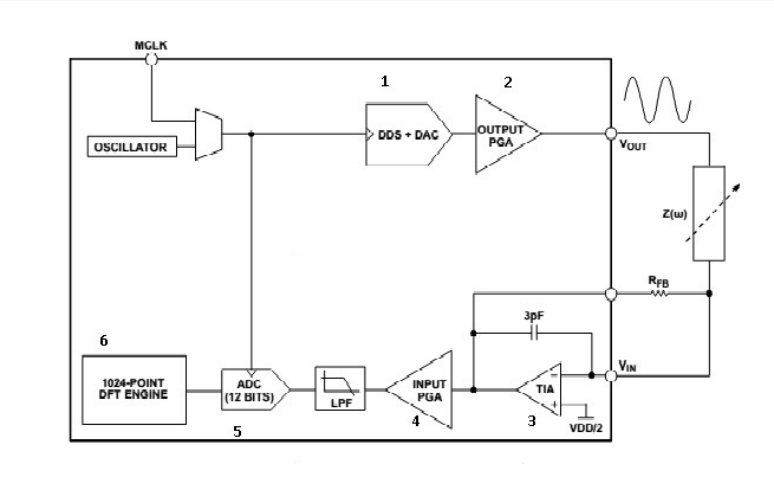

Figure 2.1 Functional block diagram of impedance measurement system [AD5933 datasheet and product info 1 MSPS].

The user has the option to power the entire circuit from the USB port of a computer. The evaluation board also has a high performance trimmed 16 MHz surface-mount crystal to act as a system clock to the AD5933, if required. Interfacing to the AD5933 is through a USB micro-controller that generates the I2C signals necessary to communicate with the AD5933 [AD5933 Evaluation Board].

The AD5933 uses a I²C bus for communication with a micro-controller. I²C bus is a synchronous bidirectional serial bus that provides an efficient method for data exchange between devices. In this system the micro-controller is the master and the AD5933 is the slave. Interfacing to the USB micro-controller is done through a Visual Basic® graphic user interface located on and run from the PC [AD5933 Evaluation Board].

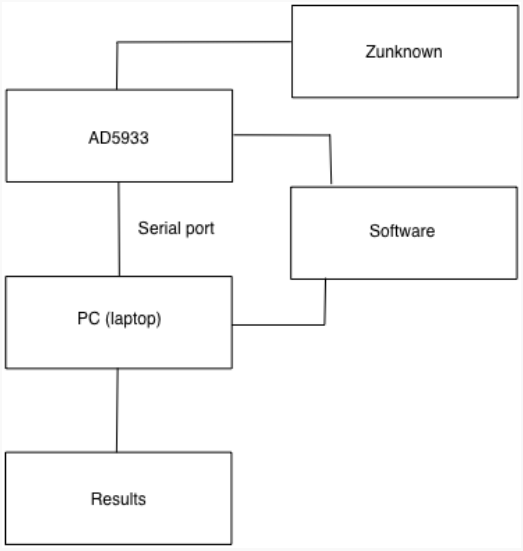

Figure 2.2 Main modules of the bio impedance measurement system.

2.2 Refractometer

Brix^0 was measured by a Hand Held ATAGO 0-32% Brix refractometer. Brix scale is a hydrometer scale for measuring the concentration of sugar content of a solution at a given temperature.

2.3 Biological materials

2.3.1 Apple and Tomato

Impedance measurement was carried out using an impedance analyzer, AD5933. The impedance measurements scanned 61 spot frequencies between 1KHz and 7KHz. A two-electrode measurement method was used. Two Ag/AgCl ECG Electrode, 30mm round (Dormo ECG Electrodes) were fixed on the skin surface of two apples and two tomatoes. Measurements were taken during ten days, seven times (17/11/2015; 18/11/2015; 19/11/2015; 21/11/2015; 24/11/2015; 25/11/2015; 27/11/2015).

2.3.2 Banana, Kiwi and Pear

The purpose of this experiment were to obtain some basic data to estimate ripening quality of banana, kiwi and pear, by capacitance properties, aiming to apply the capacitance technique to an automatic control system for the ripening of fruits. Four banana fruits from Costa Rica, three kiwis from Portugal and three “peras rocha” from Portugal were used in this experiment. The fruits have been stored between 13-16ºC temperature during nineteen days, and all the experiments were carried out at the room temperature. On the first day, bananas were at stage 3 and on the 19 day they were at stage 7 (Figure 2.3). The impedance was measured using an impedance analyzer, integrate circuit AD5933. The impedance measurements scanned 300 spot frequencies between 1KHz and 16KHz. Fruit was placed between two disc electrodes (Chloriding Ag/AgCl electrodes) of 8-mm diameter (Model E243, Warner instruments) with gel, so that impedance was measured transversely across the fruit.

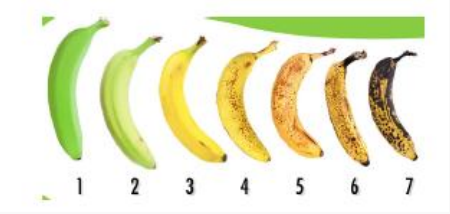

Figure 2.3 Color chart of banana fruits in various stages.

2.3.3 Grape Berries

Grape berries from one cultivars were selected for experiments. In the study four groups of berries were collected from Qta. Aguieira in five different times, between 3 of August and 15 of October. The samples were collected and stored in a plastic tube, and taken to the laboratory. Impedance spectra were acquired on AD5933 impedance analyzer with a sweep frequency between 1000Hz and 1600Hz over 300 data points. Grapes were placed between two disc electrodes (Chloriding Ag/AgCl electrodes) of 8-mm diameter (Model E243, Warner instruments) with gel, so that impedance was measured transversely across the grapes.

2.4 Measurement methods

2.4.1 Sugar measurements

Fruit flavor is fundamentally the balance between sugar and acid. Sugar content increases steadily as grape berries mature. Grape berries soluble solids, a factor highly correlated with sugar content, is an important tasting quality feature which indicates grape berries sweetness. Each grape

was used to extract fruit juice right after the electrical impedance measurement. A few drops of juice were placed on top of the prism assembly, and data were read from the graduations.

2.4.2 Impedance measurements

The impedance was measured using an impedance analyzer, AD5933. For the measurement the fruit was placed on the sensor containing conductive gel, between the fruit and electrodes. The mobile sensor support was used to prick the chloriding Ag/AgCl disk electrodes 8-mm diameter (Model E243, Warner instruments) in the fruit skin surface. Measurements were conducted at room temperature using an electrical frequency between 1KHz and 16KHz.

2.4.3 Calibration of the system

The system requires initial calibration: a precision resistor is substituted for the impedance to be measure.

The calibration of the system is done in two steps. First the gain factor is calculated from the real and imaginary parts received from AD5933. The gain factor is calculated using the equation (2.1).

$$gain\ factor = \frac{\frac{1}{imp.cal}}{Mag.} \quad \text{Equation 2.1}$$

Where imp.cal is the impedance of the R_{cal} (calibration resistor) with a known value that is used for the calibration of the system. R_{cal} should also have the same value as the R_{fb} during the calibration run. Mag is the magnitude calculated from the real and imaginary values received from the AD5933. Mag is calculated through the equation (2.2).

$$Mag = \sqrt{Img^2 + Real^2} \quad \text{Equation 2.2}$$

The phase is calculating with the formula (2.3).

$$Phase = \tan^{-1}(\frac{Img}{Real}) \quad \text{Equation 2.3}$$

To get the phase introduced only by the components between V_{in} and V_{out} all the phase data for each frequency under a calibration with a resistor has to be saved. After the measurement the phase from the calibration has to be subtracted from the phase that has been measured for each frequency. The phase is given by calculating (2.4):

$$\theta_{impedance} = \theta_{unknown} - \theta_{system} \quad \text{Equation 2.4}$$

Where θ_{system} is the phase of the system with a calibration resistor between V_{in} and V_{out}. $\theta_{unknown}$ is the total phase of the system with an unknown impedance between V_{in} and V_{out}. $\theta_{impedance}$ is the phase due to this impedance. The impedance components is given by

$$R = Z_{real} = [Z]\,cos(\theta) \quad \text{Equation 2.5}$$

$$X = Z_{imaginary} = [Z]\,sin(\theta) \quad \text{Equation 2.6}$$

Where

$$Z = R + iX$$ Equation 2.7

The phase is converted to degrees by

$$\theta = tan^{-1}(\frac{I}{R})\frac{180^{o}}{\pi}$$ Equation 2.8

The phase value ideally should be 0^{o} for a resistor and -90^{o} for a capacitor.

There are however some minor randomly distributed contributions, which can be explained taking into account that the stability of the AD5933's internal reference oscillator operated a 16.776 MHz is not perfect [Nordbotten, 2008]. Once the phase is not constant it was measured the system phase for each frequency. Because the the AD5933 has a finite frequency response, the gain factor shows a variation with frequency. This variation in gain factor results in an error in the impedance calculation over the frequency range. Figure 3.1 shows an impedance profile based on a single-point gain factor calculation. To inimize this error, the frequency sweep should be limited to a small frequency range as possible [AD5933 datasheet and product info 1 MSPS].

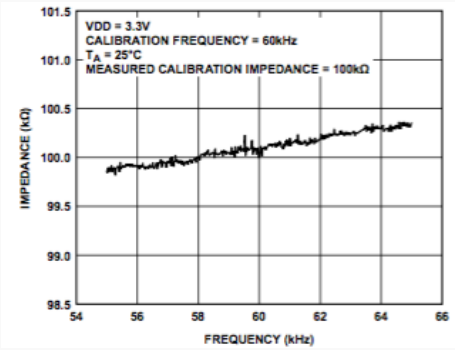

Figure 2.4 Impedance profile using a Single-point gain factor calculation [AD5933 datasheet and product info 1 MSPS].

Alternatively, it is possible to minimize this error by assuming that the frequency variation is linear and adjusting the gain factor with a two-point calibration. Figure 2.5 shows an impedance profile based on a two-point gain factor calculation [AD5933 datasheet and product info 1 MSPS].

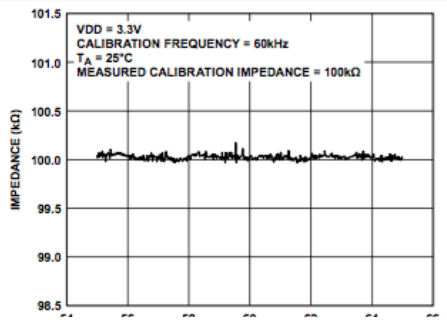

Figure 2.5 Impedance profile using a two-point gain factor calculation [AD5933 datasheet and product info 1 MSPS].

According to the EVAL AD5933EB datasheet, mid-point frequency calibration is performed for the measurement of small-scale sweeping, 2 Hz of difference, and multi-point frequency calibration is used for the measurement of large-scale sweeping. Because the PC program for multi-point frequency calibration provided by the Analog Devices Company is not accurate, mid-point frequency calibration was used in this study. According to the EVAL AD5933EB datasheet, we should choose a model with similar RC characteristics to calibrate the system. However, experiments have shown that a pure resistance model is a more accurate to calibrate the system rather than the other unknown RC models [Kicherer et., 2015].

Another important issue to be aware of is the gain factor variation with temperature, the typical error variation is 30ppm/°. Figure 2.6 shows an impedance profile with a variation in temperature for 100kΩ impedance using a two-point gain factor calibration.

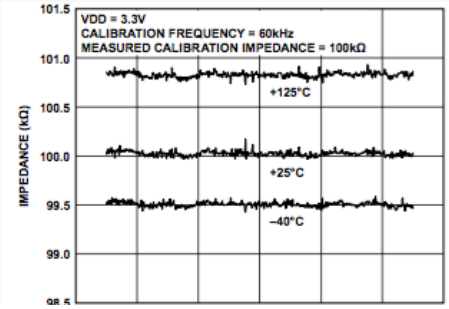

Figure 2.6 Impedance profile variation with temperature using a two-point gain factor calibration [AD5933 datasheet and product info 1 MSPS].

Table 2.1 Measurement ranges for AD5933 [Nordbotten, 2008].

Range no.	Value (KΩ)	R_{fb}(KΩ)	Cal. Resistor (KΩ)
1	0.1-1	0.1	0.1
2	1-10	1	1
3	10-100	10	10

4	100-1000	100	100
5	1000-2000	1000	1000
6	9000-10000	9000	9000

The measurement range of the system is 0.1 K to 10 M divided into six ranges as specified in table 2.1 which also gives the calibration data to be used. It is noted that the ranges 5 and 6 are a bit different from the other ranges. Range 5 goes 1 MΩ to 2 MΩ and range 6 goes from 9 MΩ to 10 MΩ. There is no range covering 2 MΩ to 9 MΩ.

Saturation phenomena that may occur during calibration and measurement is a a problem. The critical issue is the dynamic range of the ADC. This is controlled by the gain through the system as given by equation (2.9).

$$Output\ exitation\ voltage = \frac{gain\ setting\ resistor}{Z_{unkwon}} * PGA_{gain} \quad \text{Equation 2.9}$$

Through the equation is observed the gain is controlled by:

- The selected voltage for the output excitation.
- The current to voltage gain resistor (R_{fb}) in combination with the calibration resistor or during measurement $Z_{unknown}$.
- The PGA gain.

The data sheet uses calibration resistor at the lower edge of each resistor range, meaning that the ratio

$$\frac{Gain\ setting\ resistor}{Z_{unkown}(Z_{cal})} = 1 \quad \text{Equation 2.10}$$

With

$$Z_{Cal} = R_{fb} \quad \text{Equation 2.11}$$

This means that using the data sheet calibration the device measured will always have higher impedance value than the calibration resistor, and the gain setting resistor. The gain through the system will be low and the saturation of ADC will not occur. The data sheet also gives a graphical illustration of how the impedance error typically varies with frequency for measurements on resistors higher than the value of the calibration resistor. Figure 2.7 shows variation for ranges 1,2,3 and 6. For the ranges (4-6) the impedance error shows a strong increased with frequency, up to -7 and -8% for ranges 5 and 6 [Nordbotten, 2008].

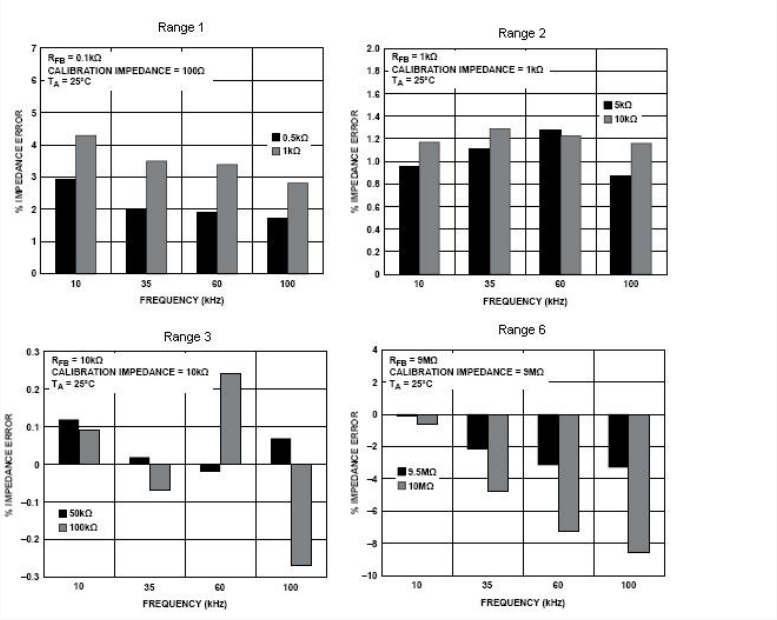

Figure 2.7 The impedance error as a function of frequency for ranges 1,2,3 and 6 [AD5933 datasheet and product info 1 MSPS].

The error seems to increase the further away from the calibration value. For range 1 the error is up to 3% all over the frequency range. Range 2 and 3 seems to give the best results. Range 2 has an error between 1-1.2% while range 3 has an error between about 0.24 to -0.27%. This illustrates that it is critical to have a calibration value close to the value of the resistor to be measured. For measurements on complex impedance there may be strong variations over the frequency span in both the imaginary part and the magnitude. The frequency run may cover more than one range. In the data sheet state that the gain factor should be calibrated when the largest response signal is present on the ADC, and the signal kept within linear range of interest. This corresponds with the conditions set in equations 1 and 2. It is also stated; the user should choose a calibration impedance which is mid value between the limits of the unknown impedance. In order to make accurate measurements a two-step calibration is needed. The first will give an approximate impedance value and the second calibration

with a calibration resistor close to the first measured value. Then the final measurement will give the most accurate value [Nordbotten, 2008].

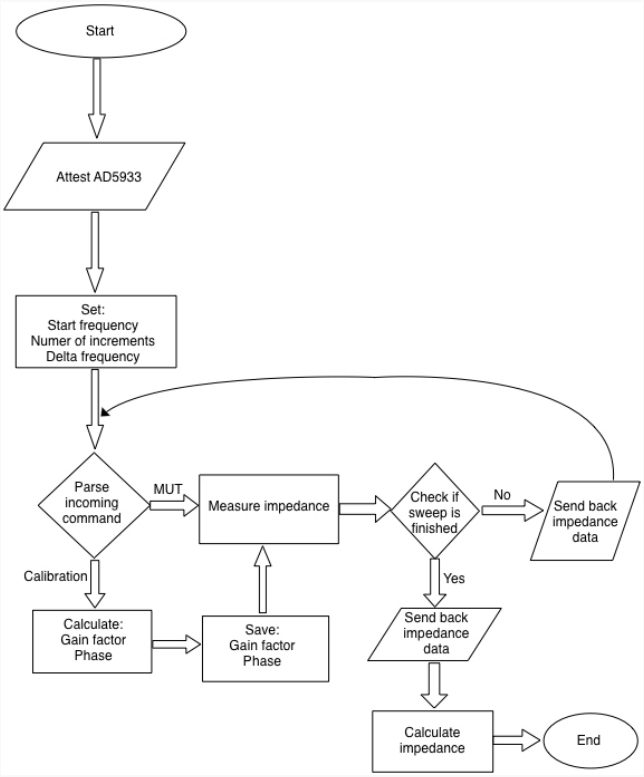

Figure 2.8 Schematic overview for impedance measurement.

2.5 Data Analysis

The csv file of impedance data obtained from each sample was exported to Excel (Microsoft Office Excel, version 2007) for organizing and prepossessing. In Excel, the imported spectra for each measurement were organized into a matrix, consisting of rows of samples and columns of variables (frequencies). Data scaling methods (table 1.1 in section 1.5.1) were used to ensure that all observations are directly comparable.

2.5.1 Multivariate analysis

PCA was performed using The Unscrambler Portable 9.7 (CAMO Inc., Oslo, Norway). The resulting data matrix was the used for multivariate data analysis. The data was analyzed in two different ways. PCA was applied to raw and normalized data.

The principal idea of this analysis is to find a structure in the data, reduce the dimensionality of the data set and identify patterns. The process starts forming a matrix with the measured elements.

Obtaining the eigenvector with the highest eigenvalues is then the principal component of the data set. Eigenvectors are then ordered by value, which again means order of significance. If the less important are left out, the final data set will have a lower dimension than the original. The score plot shows similarities and differences among the samples, allowing for pattern investigation and identification of outliers. The PLS were performed in Matlab 2014b (The Matworks Inc.,Natic, MA), with a Matlab toolbox.

2.5.2 Analysis of variance

Impedance data were explored by one-way analysis of variance (ANOVA), using fruit type or state of maturation as fixed factors. The programme used was IBM SPSS statistics. The statistical significance was set at the conventional 5% level. Differences between two variables were tested using students t-test ($p<0.05$).

3 Results and discussion

3.1 Verification tests on resistors and capacitors

For testing purposes the impedance (Z) of resistors and capacitors of known value were measured.

Resistor ($R=10^5\ \Omega$)

A resistor of 100000 Ω was measured in range 3 with the same calibration as the whole fruit measurements ($R_{FB} = R_{cal}=10^4\Omega$). The variations in [*Z*] are plotted in 3.1. Table 3.1 shows the values of impedance measured have an error <1%, and the phase angle is 0, as expected. Frequency sweep between 20000-20020 Hz was performed.

Table 3.1 Data from the system AD5933.

Frequency (Hz)	Impedance measured (Ω)	Phase^o	z0 (real)	z0 (imaginary)	Impedance calculated (Ω)	Error (%)
20000	99974	0	99974	0	100000	0.026
20002	100040	0	100040	0	100000	-0.040
20004	100024	0	100024	0	100000	-0.024
20006	100030	0	100030	0	100000	-0.030
20008	100025	0	100025	0	100000	-0.025
20010	100006	0	100006	0	100000	-0.006
20012	100020	0	100020	0	100000	-0.020
20014	100019	0	100019	0	100000	-0.019
20016	100006	0	100006	0	100000	-0.006
20018	100008	0	100008	0	100000	-0.008
20020	100003	0	100003	0	100000	-0.003

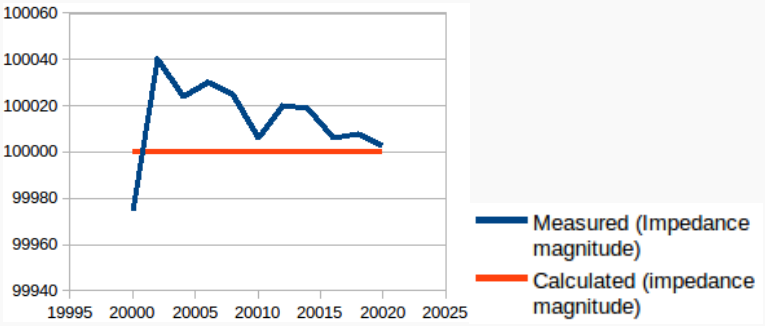

Figure 3.1 Comparison between measured and calculated impedance for resistor.

Capacitor (C= $15 * 10^{-12}$ F)

For a capacitor we have:

$$[Z] = \frac{1}{2\pi f C}$$ Equation 3.1

A capacitor of $15 * 10^{-12}$F was measured in range 3 with the same calibration as the whole fruit measurements ($R_{FB} = R_{cal}$=$10^4\Omega$). The variations in [Z] are plotted in 3.2. Table 3.2 shows the values of impedance measured have an error <5%, and the phase angle is negative, as expected. Frequency sweep between 3000-3020 Hz was performed.

Table 3.2 Data obtained from the system AD5933.

Frequency (Hz)	**Impedance measured (Ω)**	**Phase°**	**z0 (real)**	**z0 (imaginary)**	**Impedance calculated (Ω)**	**Error (%)**
30000	368598	-1.57	654.72	-368517.35	353677.65	-4.20
30002	368598	-1.57	680.47	-368554.74	353654.07	-4.21
30004	367415	-1.57	-1101.88	-367156.83	353630.50	-3.83
30006	369138	-1.57	-648.74	-368517.76	353606.93	-4.22
30008	368408	-1.57	585.23	-368517.67	353583.36	-4.22
30010	369558	-1.57	-638.33	-369924.91	353559.80	-4.63
30012	368247	-1.57	632.88	-368554.63	353536.24	-4.25
30014	366756	-1.57	1415.28	-367155.56	353512.68	-3.86
30016	367763	-1.57	-1149.28	-367156.68	353489.12	-3.87
30018	368692	-1.57	-696.33	-368517.48	353465.57	-4.26
30020	368692	-1.57	-696.33	-368517.48	353442.02	-4.27

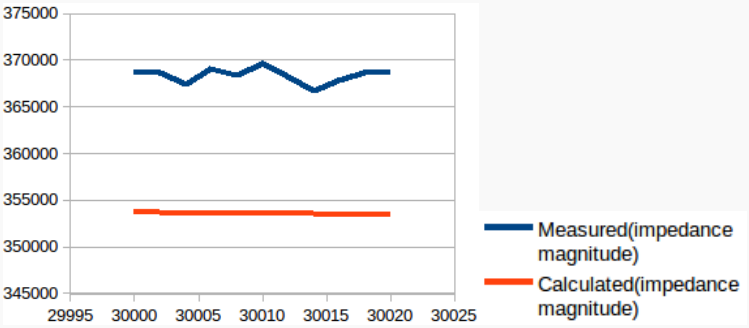

Figure 3.2 Comparison between measured and calculated impedance capacitor.

Series RC network (R= 1E5 Ω; C= $220 * 10^{-12}$ F)

A capacitor and a resistor in series were measured in range 3 with the same calibration as the whole fruit measurements ($R_{FB} = R_{cal}=10^4\Omega$). The variations in [$Z$] are plotted in 3.3. Table 3.3 shows the values of impedance measured have an error of 19%. Frequency sweep between 10000-10020 Hz was performed.

For a RC series combination, we have:

$$[Z] = \sqrt{(\frac{1}{j\omega fC})^2 + R^2} \qquad \text{Equation 3.2}$$

$$[Z] = \sqrt{Img^2 + Real^2} \qquad \text{Equation 3.3}$$

Table 3.3 Data obtained from the system AD5933.

Frequency (Hz)	Impedance measured (Ω)	Phase°	z0 (real)	z0 (imaginary)	Impedance calculated (Ω)	Error (%)
10000	100007.62	0.015	99997.08	1452.33	123424.20	19
10002	100045.76	0.015	100034.17	1522.91	123415.72	19
10004	100051.58	0.014	100041.52	1418.44	123407.24	19
10006	100128.19	0.015	100117.56	1459.40	123398.77	19
10008	100076.98	0.013	100068.02	1338.98	123390.31	19
10010	100021.81	0.014	100011.97	1403.26	123381.85	19
10012	100053.58	0.014	100043.67	1408.34	123373.39	19
10014	100023.00	0.013	100013.99	1342.41	123364.94	19
10016	99966.27	0.014	99956.91	1368.09	123356.50	19
10018	100010.00	0.015	99998.31	1528.85	123348.05	19
10020	100071.16	0.014	100060.91	1432.28	123339.62	19

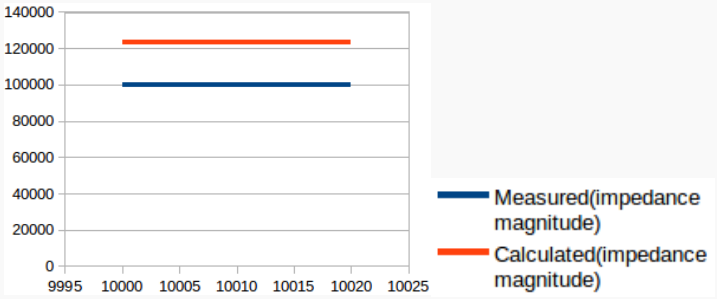

Figure 3.3 Comparison between measured and calculated impedance for series RC network.

Parallel RC network (R=2.2*10^3 3 Ω; C=2.2*10^{-10} F)

A capacitor and a resistor in parallel were measured in range 3 with the same calibration as the whole fruit measurements ($R_{FB} = R_{cal}$=10^4Ω). The variations in [Z] are plotted in 3.4. Table 3.4 shows the values of impedance measured have an error of <1%. Frequency sweep between 20000-23000 Hz was performed.

For a parallel combination, we have:

$$[Z] = \frac{R}{1+(2\pi fCR)}\sqrt{1+(2\pi fCR)^2} \qquad \text{Equation 3.4}$$

Table 3.4 Comparison between impedance measured and calculated.

Frequency (Hz)	Impedance measured (Ω)	Phase°	z0 (real)	z0 (imaginary)	Impedance calculated (Ω)	Error (%)
20000.00	2194.76	-0.058	2191.01	-128.25	2199.98	0.24
20200.00	2195.09	-0.059	2191.23	-130.10	2199.98	0.22
20400.00	2195.53	-0.060	2191.65	-130.59	2199.98	0.20
20600.00	2195.09	-0.060	2191.08	-132.53	2199.98	0.22
20800.00	2195.09	-0.061	2191.01	-133.71	2199.98	0.22
21000.00	2194.87	-0.061	2190.73	-134.73	2199.98	0.23
21200.00	2194.64	-0.062	2190.41	-136.25	2199.98	0.24
21400.00	2194.64	-0.063	2190.33	-137.48	2199.98	0.24
21600.00	2195.09	-0.063	2190.68	-139.09	2199.98	0.22
21800.00	2194.42	-0.064	2189.95	-139.93	2199.98	0.25
22000.00	2194.42	-0.065	2189.85	-141.55	2199.98	0.25

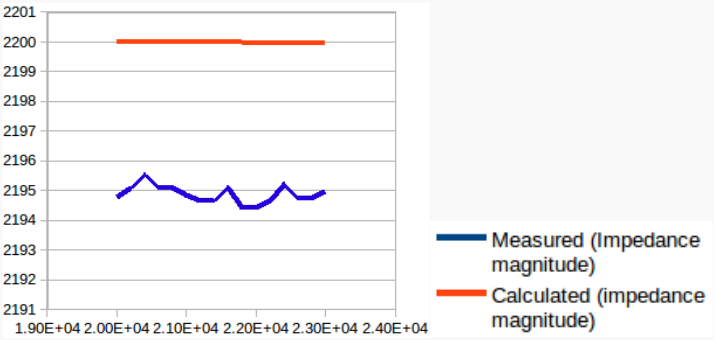

Figure 3.4 Comparison between measured and calculated impedance for parallel RC network.

3.2 Verification tests on fruit

3.2.1 Apple and tomato

The mean and the standard deviations of 20 apples and tomatoes by impedance measurements were calculated using Microsoft Excel. To investigate the system reliability, the coefficient of variation was calculated. CV was given by the formula,

$$CV = \frac{\sigma}{\mu}$$ Equation 3.5

Where μ is the mean, and σ is the standard deviation. The results are shown in Annex B. The results are from twenty measurements made in two different apples and two different tomatoes. In summary, the stability of multiple repeated experiments was good, error<1%, which showed that the system meets the measurements requirements.

3.2.1.1 Spectra analysis - raw data

Impedance, phase angle, real and imaginary parts of the fruits were calculated from the impedance analyzer data. The relationship between the impedance parameters and the frequency is described in the graphs bellow. From the measurements made during a period of time, was possible to observe a variation in the impedance parameters.

The results consist in three graphs for each fruit, Impedance Vs Frequency, maximum value of impedance and the area under curve (AUC) for each measurement. Impedance Vs Frequency plot represents the variation of impedance through different frequencies. It is also possible to observe the variation of the spectrum through the days. This plot displays the variation of impedance when subject to frequencies between 1KHz and 7KHz for 10 days. During this time, unripe apples and tomatoes became ripe.

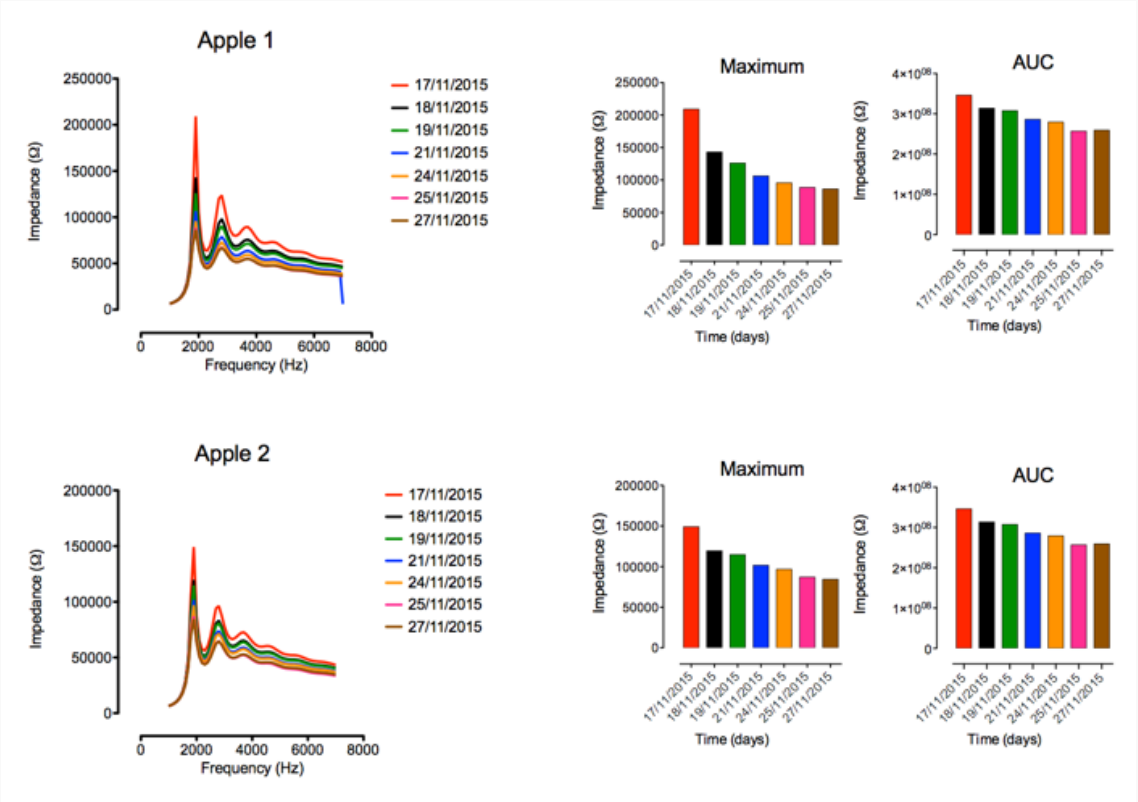

Figure 3.5 Line plot Impedance Vs Frequency of apple 1 and 2. Bar plot of maximum value of impedance for each day and bar plot of area under curve for each day.

From analysis of the characteristics shown in 3.5 is possible to conclude that apples have highest value of impedance at 1900 Hz in the frequency range of 1KHz and 7KHz. It is also observed variations in impedance from raw to ripe apple, which suggests that the maturity of apples can be reflected by impedance. Analyzing the bar plots is easy to observe the variance of impedance through the time with the maximum value of impedance than in the plot AUC, because in the higher frequencies the difference of impedance values between the days is lower. Impedance values decreases with ripening and decreases with frequency. The probable reason may be the water in the apple tissue reduces and sugar content increases. This effect is due the fact that sugar molecules can form hydrogen bonds with water dipoles, limiting its movement and decreasing its polarization capacity [Castro-Giráldez et al., 2010] The biological and biochemical studies need to be conducted parallel with the impedance studies to estimate the tissue composition changes during the ripening and the results to be correlated with impedance variation.

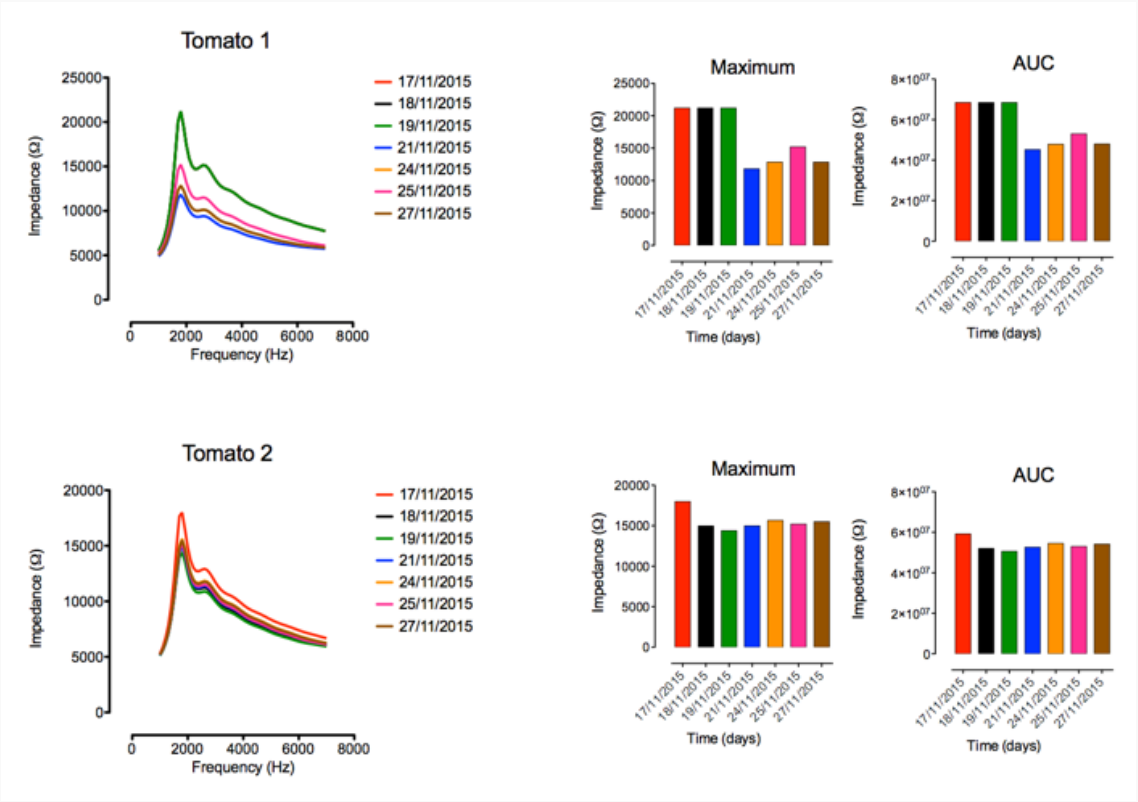

Figure 3.6 Line plot Impedance Vs Frequency of Tomato 1 and 2. Bar plot of maximum value of impedance for each day and bar plot of area under curve for each day.

Over a frequency ranging from 1KHz and 7KHz a study was executed to determine the tomatoes dielectric properties during 10 days. The results show that with increasing frequency impedance decreases, and during maturation the impedance value decrease. However, the difference of impedance values through the days is not constant. In tomato 1 during three days the impedance values did not change much instead, remained relatively constant after this period of time the impedance value decrease. Tomato 2 have a higher value of impedance in the first measurement and then the other measurements have similar values. In both tomatoes is possible to observe two groups of electric properties, one with higher impedance values and other with lower. This fact agrees with earlier reported literature regarding the main reason behind the differences in the impedance values are the structure of the cellular membranes. The tomato fruit cell wall changes during ripening. These implies that the current easily cross the fruit. Another point to state is that there are some considerable differences among the two fruits.

3.2.1.2 Multivariate analysis

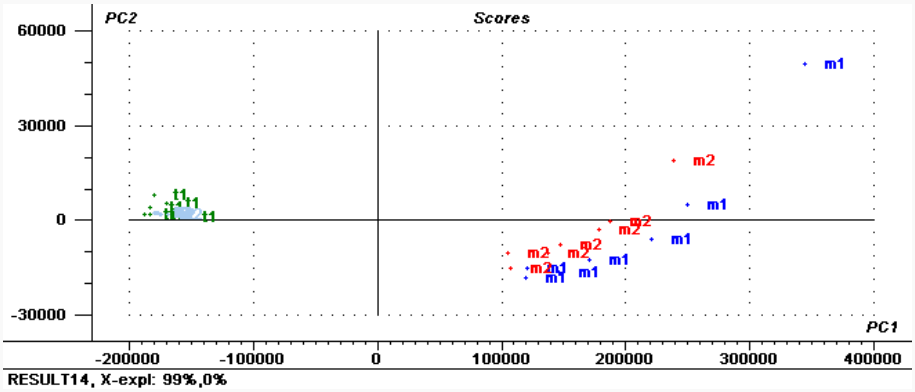

Figure 3.7 Raw data. Scores for the apples and tomatoes plotted in PC1,PC2 coordinate system.

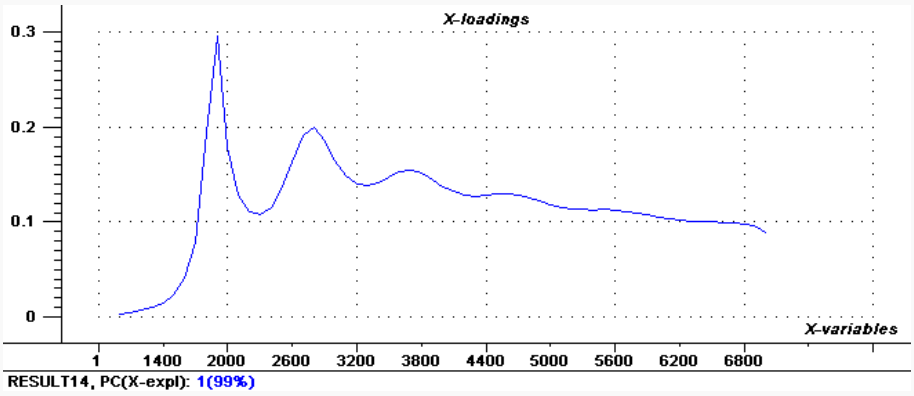

Figure 3.8 Loading plot for the PC1.

The score-plot in Figure 3.7 show a clear separation of the two fruits, suggesting that the chemical physical properties of the both fruits are different, cross the first principal component with the first two components explaining 99% of the variance. The loading plot shows that the most important frequency for the fruit separation is at 1900Hz.

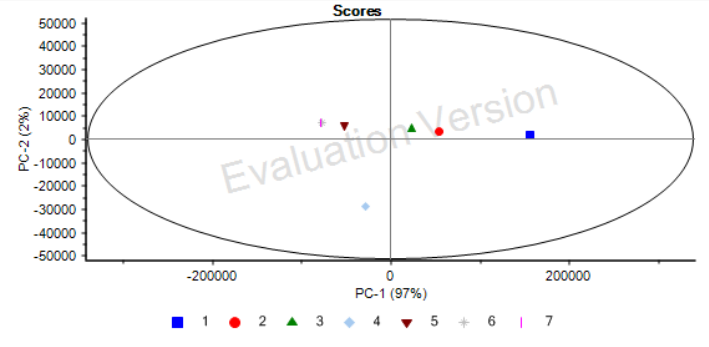

Figure 3.9 Raw data. Scores of an apple plotted in PC1 and PC2 coordinate system. The numbers correspond to an impedance measure in different days. From time 1 to time 7.

The scores plot in Figure 3.9 show a clear separation of the apple in different days. The separation in on the component 1. On the right is the first measuremt and in the left is the last measuremnt. From this plot is possible to undertsand that there is a measured componet that change while the apple is rippening.

3.3 Electrodes tests

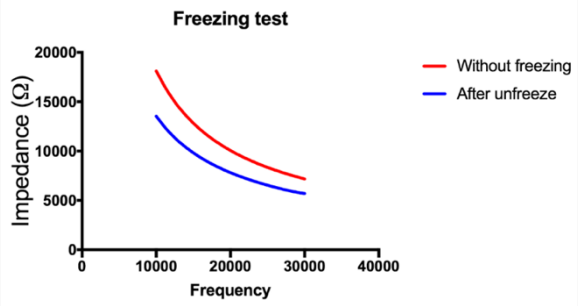

Figure 3.10 Freezing test. Impedance values of one grape before and after freeze.

In frozen storage, physical properties of food materials are generally affected by the formation of ice crystals. The electrical properties of the fruit drastically changed after freezing: impedance greatly decreased, suggesting the serious change in the cell structure. After freezing the impedance of the samples decreased across the test frequency range due to the cell damaged during the freezing process.

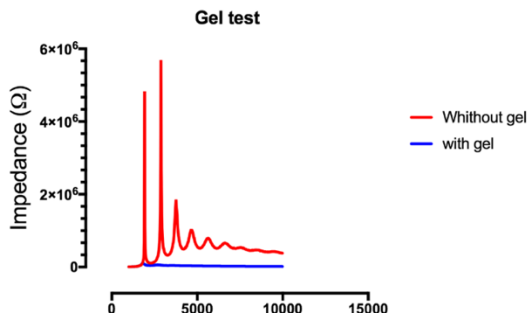

Figure 3.11 Gel test. Impedance values from a grape, measure with electrodes with gel and without gel.

The gel provides an electrolyte for efficient conductance between the Ag/AgCl electrodes and the fruit sample. In figure 3.11 is possible to observe the gel reduce the electrode-skin impedance.

3.4 Bio impedance measurements on fruit

As a result of the different mineral substances and organic acids present, along with other components susceptible to dissociation, the high electrolytic conductivity of fruits is distinguished. Impedance is an interesting parameter because dielectric properties are considered to be the most important physical properties associated with the application of different frequencies. Among the factors that are involved in the electric properties, the nature of the material that implies the composition and structure is the most common. Some other variables, such as frequency and temperature are involved with the maturity stage of the fruit. Moreover, ionic components have significant effects on the dielectric properties. Another factor is the density because the amount of mass per unit of volume has a definite effect on the interaction of the electromagnetic field and the involved mass. The ripening stage of the fruits under measure may affect the dielectric properties.

The results will be divided in three sections: grapes; banana, kiwi and pear. These three experiments were done in different times and with a different method.

3.4.1 Banana, kiwi and pear

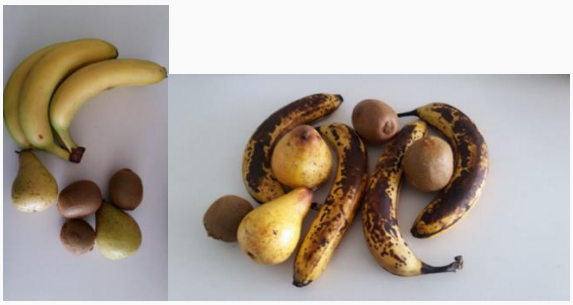

Figure 3.12 Fruits on the first day of measurements and after nineteen days.

3.4.1.1 Spectral analysis

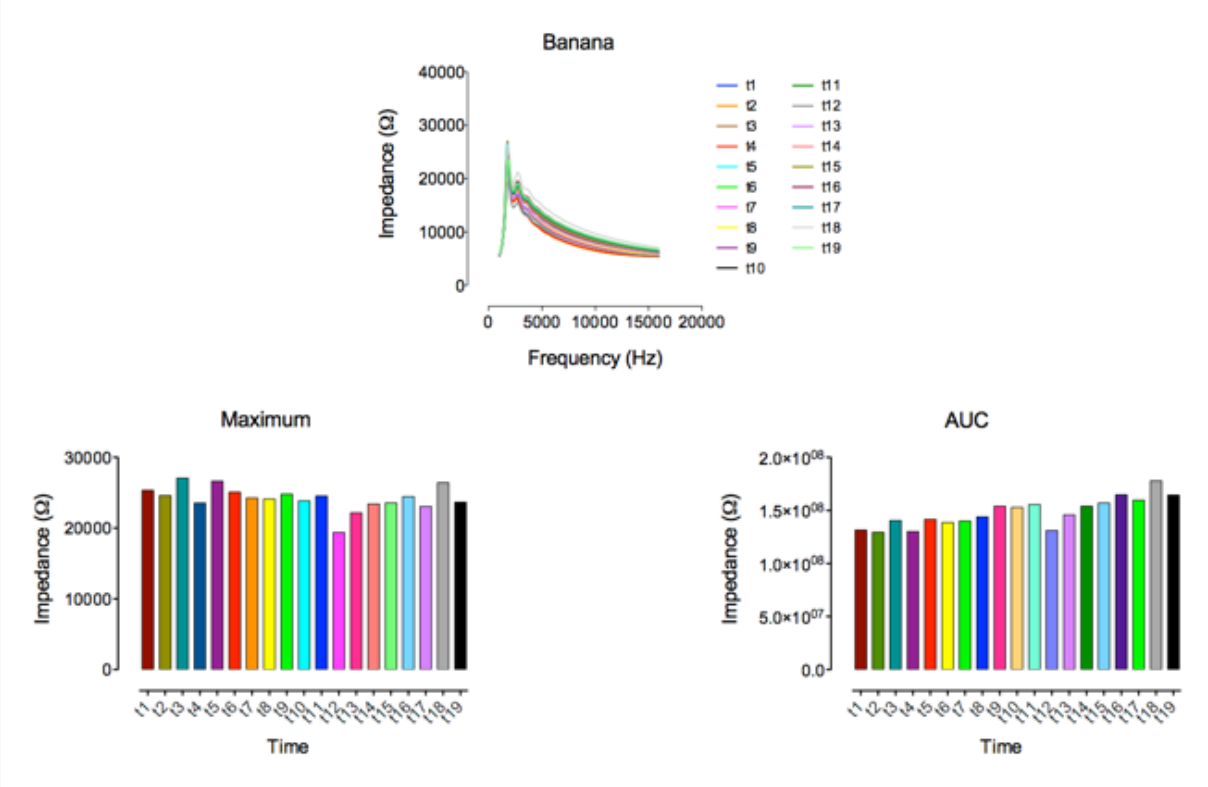

Figure 3.13 Line plot Impedance Vs Frequency of four bananas. Bar plot of maximum value of impedance for each day and bar plot of area under curve for each day.

The data obtained above are from impedance measurements in three different fruits, banana, kiwi and pear. To investigate the differences in the electrical properties of the fruit during maturation three graphs have been done. With the line plot is difficult to understand the different spectrum for each measurement so the maximum of each measurement and the area under curve was calculated. The

line plot of impedance displays the variation of impedance when subject to frequencies between 1KHz and 16KHz for 19 days. During this time, unripe bananas, kiwis and pears became ripe.

The results show that fruit impedance decrease as frequency increases. The bar plot of AUC can be used to reflect changes in banana ripening. The fruit impedance system can provide information about the state of maturation. From the AUC plot is observed that banana impedance increases during ripening. The results correspond with those obtained by Chowdhury (2015). However, if we want to have quality information about the fruit more experiments and models need to be done.

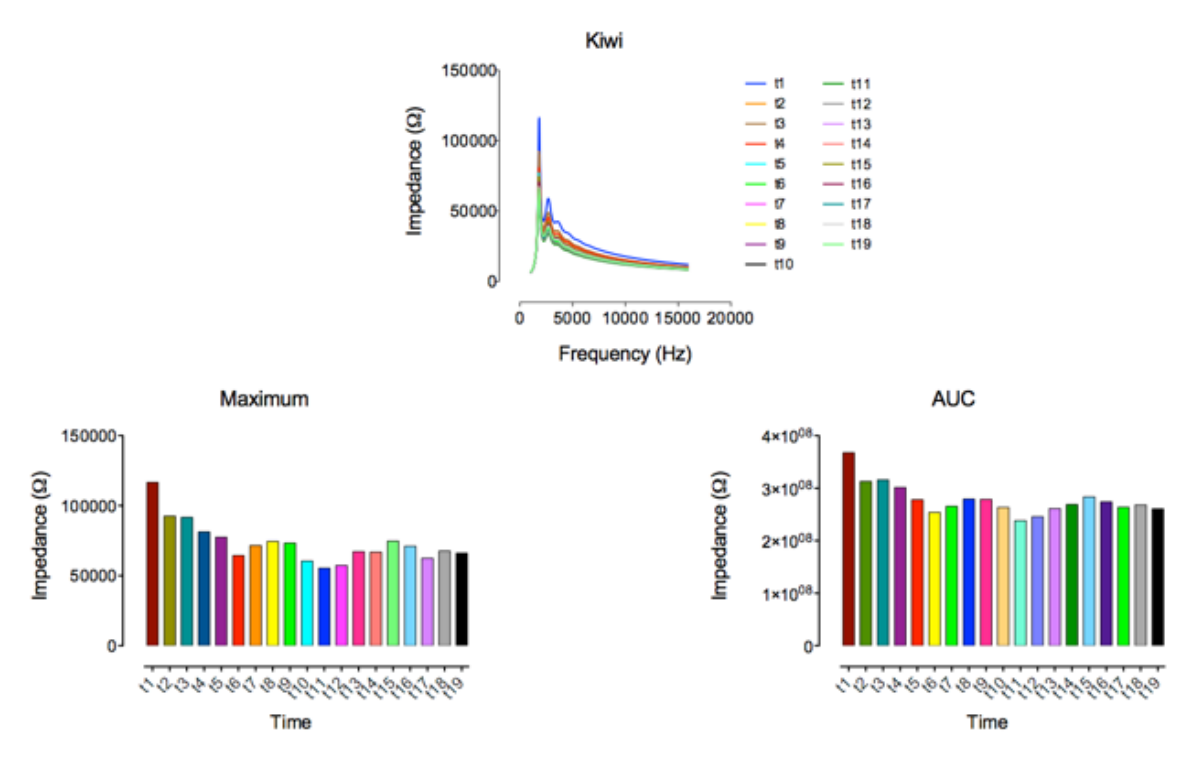

Figure 3.14 Line plot Impedance Vs Frequency of three kiwis. Bar plot of maximum value of impedance for each day and bar plot of area under curve for each day.

From the observation of the maximum bar plot, is possible to conclude that the variation of impedance through the time decrease with some fluctuations.

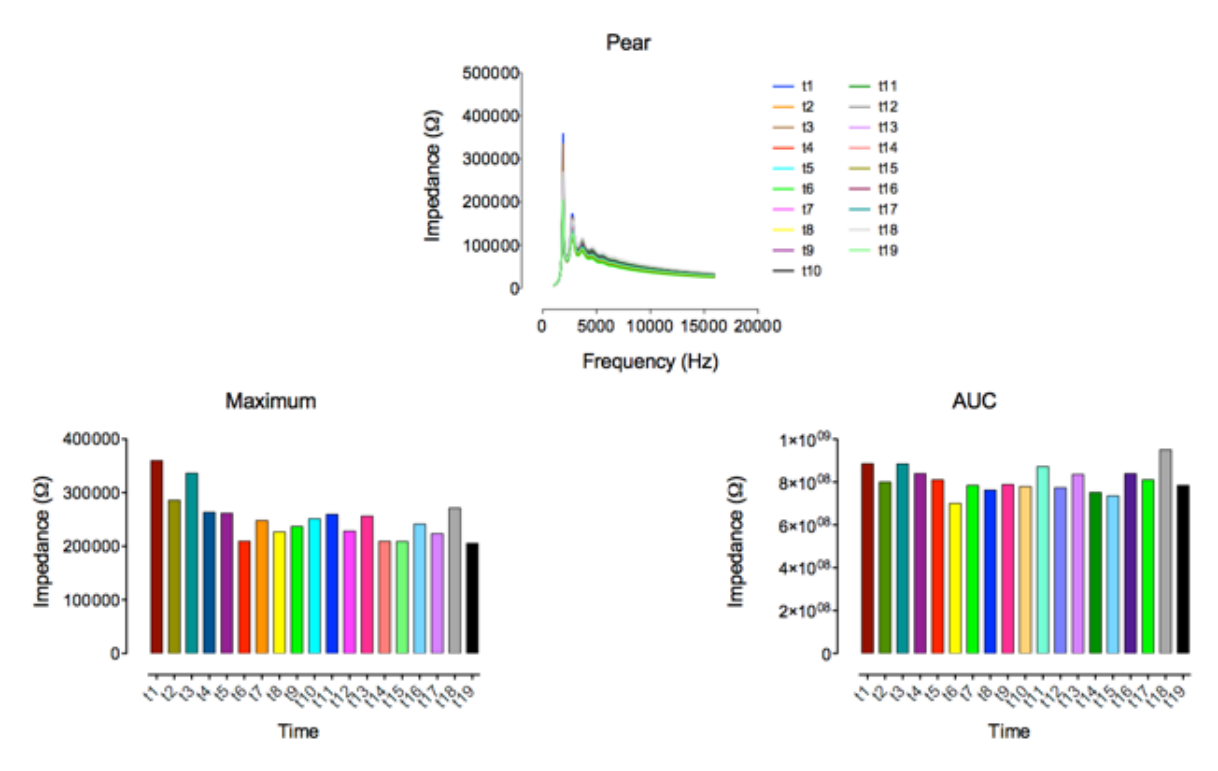

Figure 3.15 Line plot Impedance Vs Frequency of two pears. Bar plot of maximum value of impedance for each day and bar plot of area under curve for each day.

The observations reveal that the maximum and AUC bar plot did not shown a specific pattern during the ripening period. The impedance change was non-linear, and thus was not possible to judge the change of electrical properties with through the maturation.

3.4.1.2 Multivariate analysis

After the fruit measurements was completed it was used multivariate analysis with the measured results. For this it was used a program called The Unscrambler from a company named Camo. In the multivariate analysis it was used a multivariate analysis named principal component analysis, PCA.

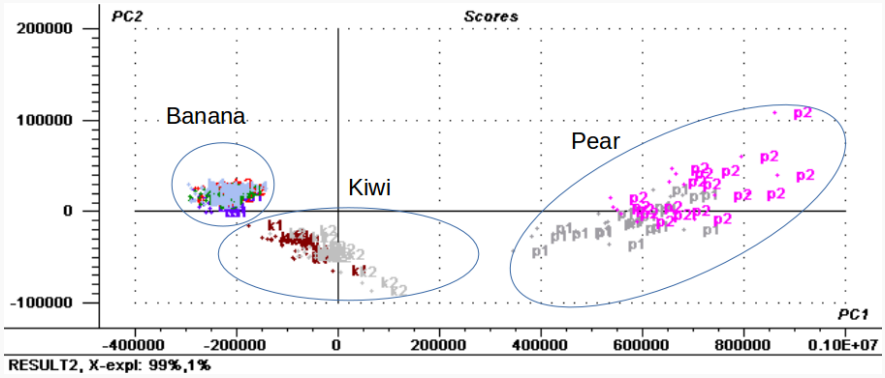

Figure 3.16 Raw data. Scores for the bananas, kiwis and pears plotted in PC1-PC2 coordinate system.

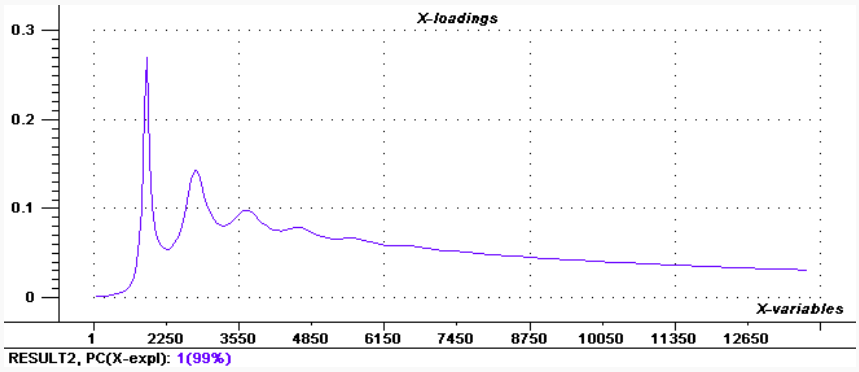

Figure 3.17 Loading plot for the PC1.

The bi-plot data of PC vs. PC2 of the raw data shows a separation between fruits. The results show that pear is highly differentiated from banana and kiwi. It is observed that the score of PC1 is much higher than the scores for PC2, and these two first principal components explain all the variance. The loading plot shows that the principal responsible for the separation of the fruits is the impedance values at 1900Hz.

Classification of data arise as signals requires a standardization step so that information extracted from biologically equivalent signals can be quantified for comparison across classes [Randolph, 2006]. In this way three data scaling methods were applied, however are only present the best results.

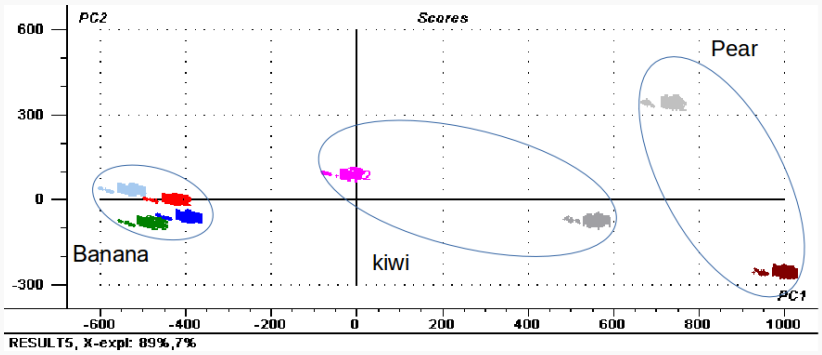

Figure 3.18 Bi-plot data of PC1 vs. PC2 from UV scaling matrix.

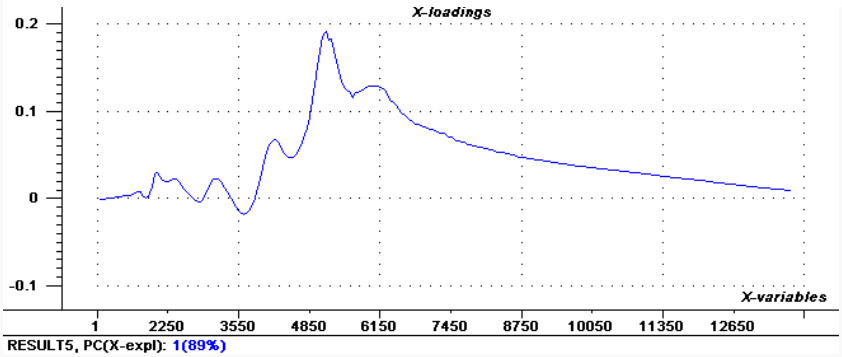

Figure 3.19 Loading plot of from UV scaling matrix.

The scores plot displays a clear separation between the three types of fruit, and also separate each fruit.

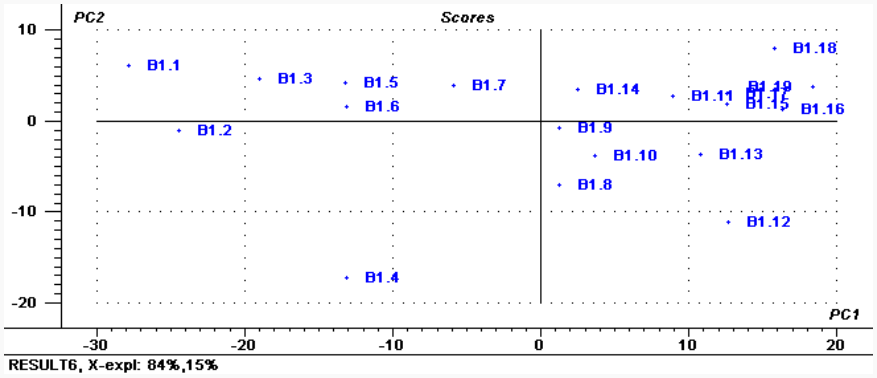

Figure 3.20 Scores of a banana plotted in PC1-PC2 coordinate system, from data normalized with uv scaling method. The numbers correspond to an impedance measure in different days. From day 1 to day 19.

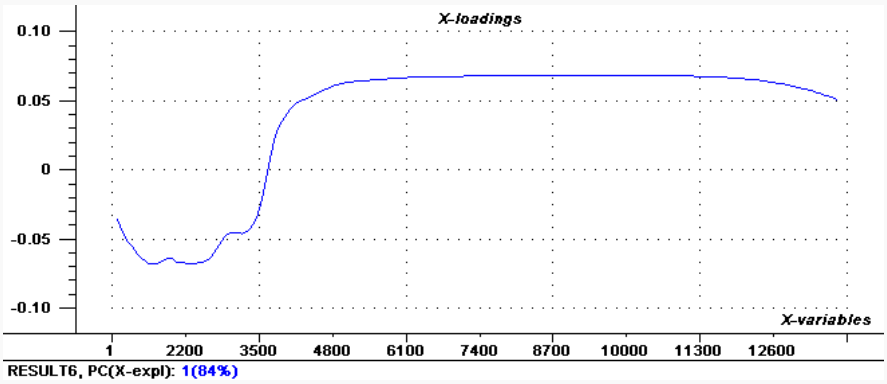

Figure 3.21 Loading plot of a banana plotted in PC1 from UV scaling matrix.

The first principal component PC1 explain 84% of the total variance. In the bi-plot, PC1-PC2 represented the evolution of the maturation, this means the transformation of the physical characteristics of the fruits, the effect is not very clear in the last days of the experiment.

3.4.1.3 Analysis of variance

In order to investigate if there are a statistically difference between the fruits, an analysis of variance was performed. From the PCA loading was concluded that the most significant variable to distinguish between the fruit was the frequency 1900 Hz, so the ANOVA was performed with the impedance values from this frequency.

The first test was the ANOVA One Way.

Table 3.5 Descriptive results.

Descriptive Statistics

Dependent Variable: 1900

fruta	Mean	Std. Deviation	N
banana	22788,4079	2387,51751	76
pear	251855,632	56640,6336	38
kiwi	61424,0263	11885,9300	38
Total	89714,1184	99475,1830	152

From this table is possible to observe a difference between the mean of each fruit. The standard deviation also present differences in each fruit.

Table 3.6 Test of homogeneity of variances. Levene statistic.

Test of Homogeneity of Variances

1900

Levene Statistic	df1	df2	Sig.
54,197	2	149	,000

With the Levene statistic we conclude the Std.deviations for each group are statistically different, sig < 0.05.

Table 3.7 ANOVA results .

Tests of Between-Subjects Effects

Dependent Variable: 1900

Source	Type III Sum of Squares	df	Mean Square	F	Sig.	Partial Eta Squared	Noncent. Parameter	Observed Power[b]
Corrected Model	1,370E+12[a]	2	6,849E+11	820,645	,000	,917	1641,291	1,000
Intercept	1,717E+12	1	1,717E+12	2056,910	,000	,932	2056,910	1,000
Fruit	1,370E+12	2	6,849E+11	820,645	,000	,917	1641,291	1,000
Error	1,244E+11	149	834608563					
Total	2,718E+12	152						
Corrected Total	1,494E+12	151						

a. R Squared = ,917 (Adjusted R Squared = ,916)

b. Computed using alpha =

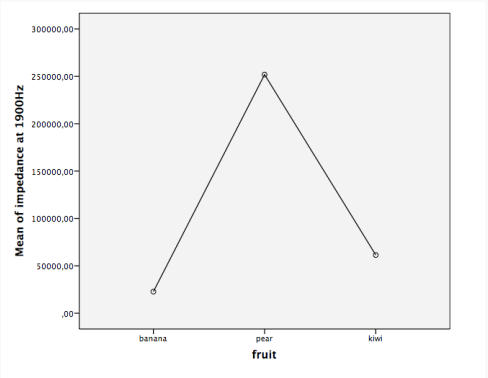

Figure 3.22 Means plot.

From ANOVA is possible to conclude that there is a statistical difference somewhere between groups. From the mean plots we observe that the most different fruit is the pear. The values of Partial Eta Squared indicate that 91.7% of the variability of impedance is comes from group membership, in this case fruit type. To analyze each group post-hoc test was performed.

Table 3.8 Post-hoc test.

Multiple Comparisons

Dependent Variable: 1900

Tukey HSD

(I) fruta	(J) fruta	Mean Difference (I-J)	Std. Error	Sig.	95% Confidence Interval	
					Lower Bound	Upper Bound
banana	pear	-229067,2*	5739,78004	,000	-242655,40	-215479,05
	kiwi	-38635,62*	5739,78004	,000	-52223,793	-25047,443
pear	banana	229067,22*	5739,78004	,000	215479,049	242655,399
	kiwi	190431,61*	6627,72710	,000	174741,332	206121,878
kiwi	banana	38635,618*	5739,78004	,000	25047,4434	52223,7934
	pear	-190431,6*	6627,72710	,000	-206121,88	-174741,33

Based on observed means.
The error term is Mean Square(Error) = 834608563,290.
*. The mean difference is significant at the

We can see from Table 3.8, that the mean scores from frequency 1900 Hz were statistically significantly different between the three fruits, sig<0.05.

3.4.2 Grapes

EIS has been applied on indication of grape ripening. Grapes from four different times where analyzed. The impedance was measured for a group of grapes from each day.

The grapes from the second day were in the period when the color change (veraison). In this way the grapes were separated in three different groups by color. Letter “p” represent the black grapes, “m” the grapes that are changing the color, and “b” the green grapes. Berry with different pigmentation was analyzed by measuring impedance.

Figure 3.23 Grapes in the same stage of maturation, with different pigmentation.

3.4.2.1 Multivariate analysis

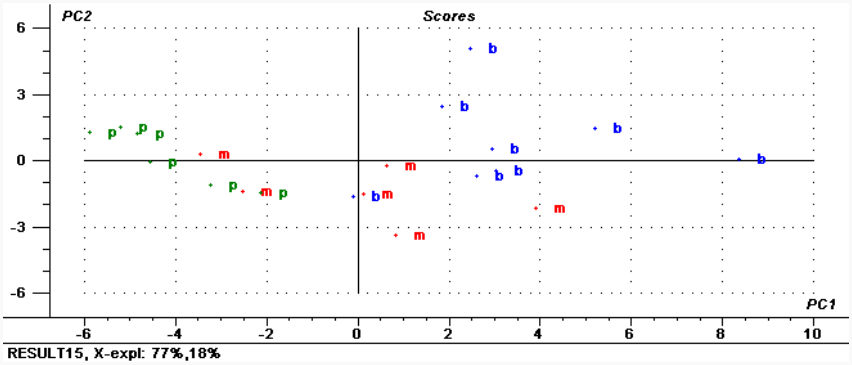

Figure 3.24 Scores on PC1-PC2 obtained by impedance data with pareto scaling. Samples are represented by letters: "p" represent the black grapes, "m" the grapes that are changing the color, and "b" the green grapes.

Figure 3.24 shows the scores of impedance data on the first two principal components. It is possible to notice that the first principal componet, which is the direction of maximum explained variance (95%), demonstrates a satisfatory, although incomplete, separation between the three groups of grapes.

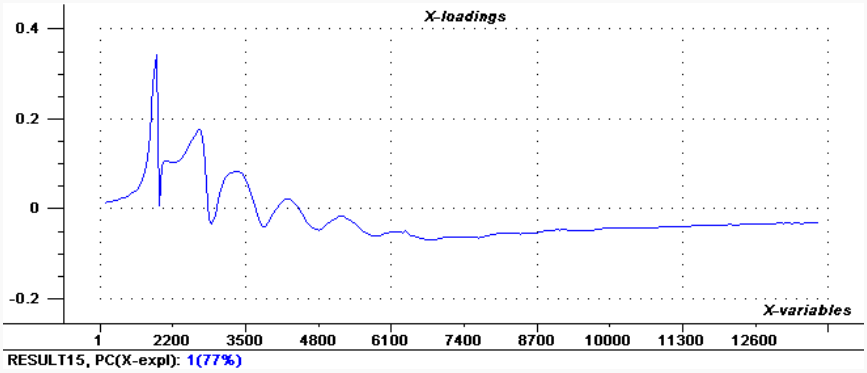

Figure 3.25 Loading from impedance spectra with pareto scaling.

The loading plot shows that the principal responsible for the separation of the grapes is the impedance values at 1900Hz.

The unsupervised nature of the PCA algorithm only reveals group structure when within-group variation is sufficiently less than between group variation. The supervised forms of discriminate analysis such as Partial Least Squares (PLS) rely on the class membership of each observation, a predict model was developed and tested based on the samples. In this way, the impedance of the grapes from each day were measured and a matrix with the group classification were prepared to introduce in the

Unscrambler portable 9.7 software. PLS regression with cross-validation was used in order to compare the predictive ability as a function of the number of components included.

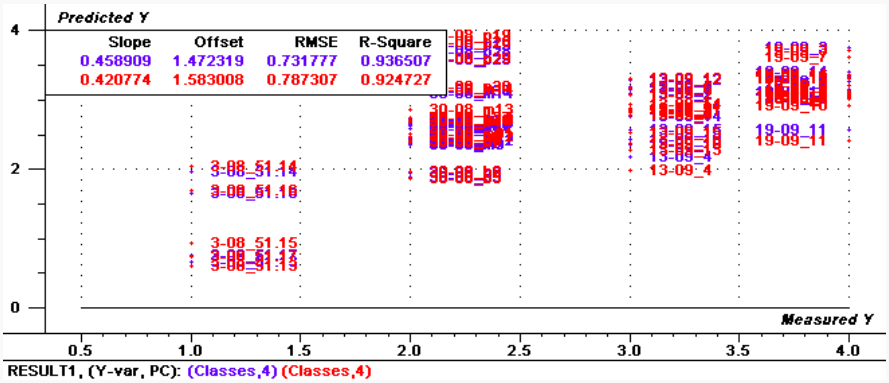

Figure 3.26 Predicted versus measured impedance values.

The R^2 is a statistical measure of how well a regression line approximates the real data points, an R^2 of 1 represents a perfect fit. RMSE is the Root Mean Square Error. It is expressed as average modeling error in the same units as the original response values. The very high value 0.93, obtained with 4 principal components both for fitting and prediction clearly demonstrate the potential of the technique. Nevertheless, more samples are needed to provide the desired robustness for classification power avoiding over fitting.

PLS-R was used in order to find the relation between the impedance data and Brixº. The ability of bio impedance spectroscopy to correlate with Brixº has been reported [(Fang et al., 2007]. For this purpose grapes from different days and state of maturation were analysed and calibration model has been developed by applying partial least-squares (PLS) regression to impedance data. The statistical indicators used to evaluate the model were root mean square error of cross validation (RMSECV), root mean square error of calibration (RMSEC) and coefficient of determination (R^2). RMSECV describes the predictive accuracy of the calibration model in relation to the reference data. RMSEC gives an indication of the average prediction error obtained for several samples. R^2 is the ratio of the explained variation to the total variation.

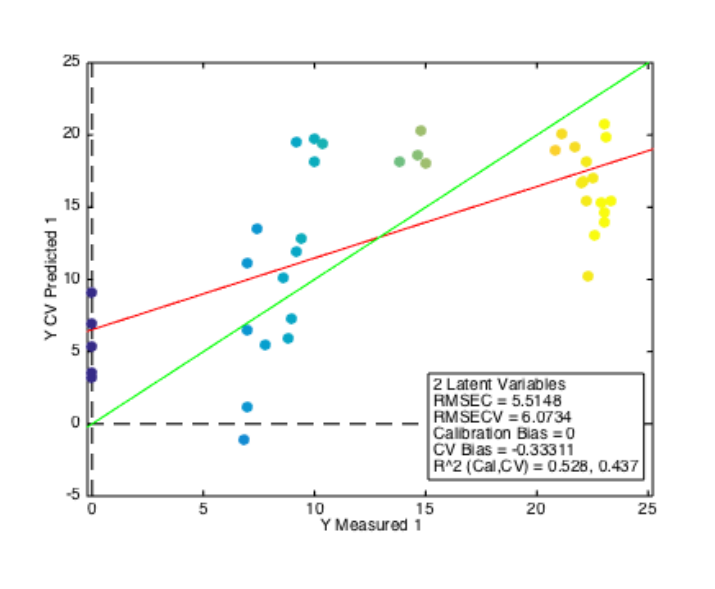

Figure 3.27 Partial least-squares cross validation for measurement of Brixº using impedance spectroscopy.

Figure 3.27 shows the predict Brixº compared with the impedance measured values. Results from this study showed that the calibration statistics were good for Brixº, with a coefficient of determination (R^2)= 52.8%. The low differences between RMSEC (5.5148) and RMSECV (6.0734) values show that the built models are near to the real situatuins of the samples set. The number of latent variables for this calibration model was 2. Grapes (n = 40) belonging to different days were analysed and quantified by Brixº. Spectra obtained by bio impedance were correlated with these values by use of PLS regression. Although, the number of samples was small it has been concluded that impedance spectroscopy can be used as an easy and rapid tool to classify the grapes according to the state of maturation.

4 Conclusions

Today, many attempts to use impedance measurement in food technology show fast success in research but industrial application remains rare. In the present study, the simple and portable AD5933 EVAL sensor was studied. The system enables the fast measurement of different fruit impedance in a nondestructive way. The identification of differences in impedance values between different fruit and stages of maturation show the feasibility of this sensor. However, some of the experiments do not show the expected results.

Electrical impedance measurements aiming to discriminate cross products have been conducted in three different fruits, banana, kiwi and pear. It was noticed that impedance spectra is a reliable method for fruit characterization.

This study highlights the physiological changes of bananas during the ripening process through the use of impedance measurement. A positive linear relationship between impedance and ripening was observed for the banana fruit. The composition change of the banana tissue may be the principal factor that account for those results. Conversely, kiwi and pear did not show a linear relationship between impedance and stage of maturity. This was unexpected since the study with other fruits have shown a considerable correlation between impedance and ripening. The failure to observe any impedance linear variation was checked using different multivariate analysis of data, and scaling methods. The results suggested that the properties that influence the impedance values did not change during kiwi maturation. The failure in pear fruit can be explained by the presence of chemical products added during the harvest, which prevents the pear maturation.

The preliminary experiments in fruit showed that all of the impedance values of the different fruits have the same behavior with respect to frequency. Additionally, the decline in the impedance value is notable characteristic with the increasing frequency.

The study with grapes has shown the capability of electric impedance to characterize grapes with different maturity stages and chemical characteristics. The grapes with different pigmentation were successfully divided in three different groups. The grapes from four times of maturation presented a model that can be used to predict the maturation phase namely green; veraison; post-veraison and mature of the grapes. A calibration model has been developed to predict Brixº in grapes. Although the number of samples was small and not enouth to have a good calibration model, it was observed the possibility of the sensor to classify the grapes according to the Brixº, more tests need to be done in order to understand how many groups of classification can be stablished and with what certainty. The results showed that the impedance spectra can be used to reflect changes in grape maturation.

The study concludes that information provided by dielectric properties can be useful in developing a non-destructive method for detecting internal fruit quality. However, if we want to measure the quantitative indicators of the fruit maturation further experiments are required to obtain to obtain reliable data in order to establish a model.

5 Future work

The basic principles of the system are very promising, even though the functionality needs further improvements. By facing the expected difficulties lead to learn about problems have also given some ideas on possible improvements, using different hardware, or improving the integrate circuit. The software used during this work was the one given by analog devices, the development of a new software for the impedance fruit measurements is an important improvement of the system.

The preliminary experiments for monitoring fruit ripening showed that the impedance was related with physical parameters of fruit, that change during maturation. To control all the maturation, process all further experiments are required for practical use. For future work an increased number of samples will need to be analyzed and the measurements need to be conducted parallel with the biological and biochemical studies to estimate the tissue composition changes during the ripening.

Micro controller based system can be developed leading to the arising mobile devices suited to select/pluck the fruits from the field to the consumer cross the entire value chain.

6 Annex

Annex A

Complex numbers

Complex numbers represent points in s-plane (Figure 1.5) that are referenced to two distinct axis. The horizontal axis is called the “real axis” and the vertical axis is called the “imaginary axis”.

$$Z = B + jA \qquad \text{Equation 6.1}$$

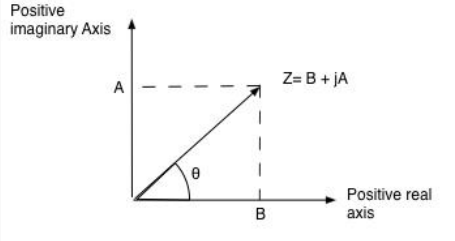

Figure 6.1 Complex s-plane representation of impedance.

Another representation is the polar form. Is based in the triangular form (Figure 1.6), it use the geometry of the triangle, Pythagoras’s Theorem, on triangles to find both the magnitude and the angle of the complex number. Thus, a polar form vector is presented as: $Z = A\angle(\theta)$, where: Z is the complex number in polar form, A is the magnitude or modulo of the vector and (θ) is its angle or argument of A which can be either positive or negative. The magnitude and angle of the point still remains the same as for the rectangular form above, this time in polar form the location of the point is represented in a “triangular form” as shown in figure (1.5) [Basic Electronics Tutorials].

$$A^2 = X^2 + Y^2 \qquad \text{Equation 6.2}$$

$$A = \sqrt{X^2 + Y^2} \qquad \text{Equation 6.3}$$

$$X = A.cos(\theta) \qquad \text{Equation 6.4}$$

$$\mathrm{Y} = \mathrm{A}.\sin(\theta) \qquad \text{Equation 6.5}$$

$$\theta = tan^{-1}(\frac{Y}{X})$$ Equation 6.6

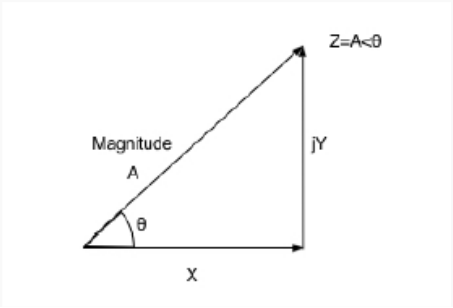

Figure 6.2 Polar form representation of a complex vector.

Annex B

Table 6.1 Standard deviations of 20 apples and tomatoes.

	Apple 1			Apple 2			Tomato 1			Tomato 2		
Frequency (Hz)	Mean	SD	%	Mean	SD	%	Mean	SD	%	Mean	SD	%
1000.00	6428.14	1.84	0.03	6395.80	2.45	0.04	4972.00	14.28	0.29	5119.34	3.02	0.06
1100.00	7487.28	1.72	0.02	7445.44	3.91	0.05	5319.25	13.97	0.26	5568.77	3.77	0.07
1200.00	8933.55	2.28	0.03	8879.35	5.42	0.06	5827.34	14.27	0.24	6199.95	4.26	0.07
1300.00	10974.43	2.90	0.03	10908.68	8.97	0.08	6537.84	15.13	0.23	7077.97	5.67	0.08
1400.00	14009.52	4.48	0.03	13940.09	12.19	0.09	7525.70	17.12	0.23	8314.80	7.56	0.09
1500.00	18846.96	7.69	0.04	18797.91	18.30	0.10	8872.90	20.52	0.23	10041.26	11.37	0.11
1600.00	27377.49	13.28	0.05	27434.03	29.27	0.11	10517.85	27.72	0.26	12200.85	19.57	0.16
1700.00	44850.51	41.93	0.09	45250.33	67.12	0.15	11967.47	37.94	0.32	14084.96	33.10	0.23
1800.00	87039.78	146.08	0.17	86805.54	353.24	0.41	12439.38	45.63	0.37	14542.41	42.20	0.29

1900.00	125633.01	327.49	0.26	111973.04	1173.25	1.05	11951.50	46.65	0.39	13721.89	41.21	0.30
2000.00	83912.37	90.55	0.11	75785.60	585.92	0.77	11157.13	43.76	0.39	12620.72	35.91	0.28
2100.00	62773.42	58.64	0.09	57980.70	347.30	0.60	10481.29	40.53	0.39	11752.70	31.32	0.27
2200.00	54693.92	45.07	0.08	51062.88	277.73	0.54	10024.30	38.65	0.39	11199.66	28.88	0.26
2300.00	53213.74	53.04	0.10	49900.12	263.23	0.53	9783.66	37.47	0.38	10927.95	28.47	0.26
2400.00	55991.26	54.81	0.10	52493.61	288.08	0.55	9713.68	38.00	0.39	10865.43	28.70	0.26
2500.00	63086.20	80.11	0.13	58795.31	356.84	0.61	9758.74	38.86	0.40	10929.75	30.06	0.28
2600.00	74084.98	96.38	0.13	68079.53	498.02	0.73	9818.05	40.09	0.41	10988.76	31.21	0.28
2700.00	85626.44	127.78	0.15	76832.32	666.18	0.87	9787.09	41.41	0.42	10921.59	32.23	0.30
2800.00	90138.84	129.83	0.14	79258.24	759.40	0.96	9635.74	41.62	0.43	10705.15	31.74	0.30
2900.00	84967.07	117.95	0.14	74543.46	698.12	0.94	9404.15	41.29	0.44	10400.67	30.39	0.29
3000.00	76514.46	82.39	0.11	67631.47	614.69	0.91	9147.84	40.26	0.44	10077.09	28.95	0.29
3100.00	69759.37	66.80	0.10	62164.89	510.73	0.82	8910.02	39.42	0.44	9784.53	27.89	0.29
3200.00	65950.61	61.22	0.09	59049.00	465.37	0.79	8709.00	38.42	0.44	9542.22	26.64	0.28
3300.00	64861.86	70.94	0.11	58110.03	441.24	0.76	8555.04	37.79	0.44	9359.75	26.21	0.28
3400.00	65779.76	68.50	0.10	58764.39	455.56	0.78	8442.00	37.50	0.44	9227.29	25.73	0.28
3500.00	68111.71	71.99	0.11	60523.71	502.66	0.83	8362.14	37.38	0.45	9129.55	25.54	0.28
3600.00	70481.26	80.69	0.11	62176.16	531.37	0.85	8282.44	37.37	0.45	9028.09	25.94	0.29
3700.00	71393.06	97.83	0.14	62633.25	562.90	0.90	8181.52	37.59	0.46	8899.08	25.32	0.28

3800.00	70154.26	66.01	0.09	61456.61	542.82	0.88	8057.14	37.20	0.46	8742.58	24.64	0.28
3900.00	67533.18	65.43	0.10	59265.00	516.16	0.87	7918.35	36.79	0.46	8572.98	24.14	0.28
4000.00	64452.63	55.71	0.09	56766.73	480.58	0.85	7776.43	36.24	0.47	8402.11	23.25	0.28
4100.00	62009.20	48.54	0.08	54761.85	459.66	0.84	7646.55	35.72	0.47	8246.86	22.61	0.27
4200.00	60406.91	59.94	0.10	53419.10	443.76	0.83	7527.84	35.07	0.47	8106.76	22.02	0.27
4300.00	59852.50	48.06	0.08	52908.78	431.75	0.82	7425.86	34.73	0.47	7987.38	21.50	0.27
4400.00	59969.06	51.38	0.09	52908.07	432.79	0.82	7340.71	34.63	0.47	7887.05	21.53	0.27
4500.00	60413.11	61.41	0.10	53157.29	464.47	0.87	7264.50	34.60	0.48	7795.63	21.29	0.27
4600.00	60550.81	54.69	0.09	53162.34	461.78	0.87	7187.49	34.29	0.48	7701.61	20.60	0.27

7 Bibliography

1) AC inductor circuits. Available: http://www.electronicsteacher.com/alternating-current/reactance-and-impedance-inductive/ac-inductor-circuits.php.
2) AD5933 datasheet and product info 1 MSPS, 12 Bit Impedance Converter Network Analyzer Analog Devices. Available: http://www.analog.com/en/products/rf-microwave/direct-digital-synthesis-modulators/ad5933.html.
3) AD5933 Evaluation Board Analog Devices. Available: http://www.analog.com/en/design-center/evaluation-hardware-and-software/evaluation-boards-kits/eval-ad5933.html#eb-overview.
4) Basic Electronics Tutorials and Revision. Available: http://www.electronics-tutorials.ws/.
5) Lessons in Electric Circuits — Volume II (AC) Chapter 4. Available: http://ieeebooks.blogspot.pt/2011/02/lessons-in-electric-circuits-volume-ii_5735.html.
6) Meftah Salem M. Alfatni, Abdul Rashid Mohamed Shariff, Mohd Zaid Abdullah, Mohammad Hamiruce B. Marhaban, Osama M. Ben Saaed. The application of internal grading system technologies for agricultural products — Review. *Journal of Food Engineering*, 116(3):703—725, 2013.
7) Anne D Bauchot, F. Roger Harker, W. Michael Arnold. The use of electrical impedance spectroscopy to assess the physiological condition of kiwifruit. *Postharvest Biology and Technology*, 18(1):9—18, 2000.
8) L. Caravia, C. Collins, S.D. Tyerman. Electrical impedance of Shiraz berries correlates with decreasing cell vitality during ripening: Impedance of Shiraz berries and cell vitality. *Australian Journal of Grape and Wine Research*, 21(3):430—438, 2015.
9) M. Castro-Giráldez, P.J. Fito, M.D. Ortolá, N. Balaguer. Study of pomegranate ripening by dielectric spectroscopy. *Postharvest Biology and Technology*, 86:346—353, 2013.
10) Marta Castro-Giráldez, Pedro J. Fito, Creu Chenoll, Pedro Fito. Development of a Dielectric Spectroscopy Technique for Determining Key Chemical Components of Apple Maturity. *Journal of Agricultural and Food Chemistry*, 58(6):3761—3766, 2010.
11) Ana M. Cavaco, Pedro Pinto, M. Dulce Antunes, Jorge Marques da Silva, Rui Guerra. \textquoteleftRocha' pear firmness predicted by a Vis/NIR segmented model. *Postharvest Biology and Technology*, 51(3):311—319, 2009.
12) Chowdhury, T. K. Bera, D. Ghoshal, B. Chakraborty. Studying the electrical impedance variations in banana ripening using electrical impedance spectroscopy (EIS). *Computer,*
13) *Communication, Control and Information Technology (C3IT), 2015 Third International Conference on*:1—4, 2015.

14) D. Cozzolino, W. Cynkar, N. Shah, P. Smith. Technical solutions for analysis of grape juice, must, and wine: the role of infrared spectroscopy and chemometrics. *Analytical and Bioanalytical Chemistry*, 401(5):1475—1484, 2011.
15) Hassan R. El-Ramady, Éva Domokos-Szabolcsy, Neama A. Abdalla, Hussein S. Taha, Miklós Fári. Postharvest Management of Fruits and Vegetables Storage. In *Sustainable Agriculture Reviews* (Lichtfouse, Eric, ed.). Springer International Publishing, 2015.
16) Q. Fang, X. Liu, I. Cosic. Bioimpedance Study on Four Apple Varieties. In *13th International Conference on Electrical Bioimpedance and the 8th Conference on Electrical Impedance Tomography* (Scharfetter, Hermann and Merwa, Robert, ed.). Springer Berlin Heidelberg, 2007.
17) Meredith Damien Gall, Walter R. Borg, Joyce P. Gall. *Educational research: An introduction.* Longman Publishing, 1996.
18) Jim Giovannoni. Molecular Biology of Fruit Maturation and Ripening. *Annual Review of Plant Physiology and Plant Molecular Biology*, 52(1):725—749, 2001.
19) F. Roger Harker, Shelley K. Forbes. Ripening and development of chilling injury in persimmon fruit: an electrical impedance study. *New Zealand Journal of Crop and Horticultural Science*, 25(2):149—157, 1997.
20) Phillipa J. Jackson, F. Roger Harker. Apple bruise detection by electrical impedance measurement. *HortScience*, 35(1):104—107, 2000.
21) D. Jamaludin, S. Abd Aziz, N. U. A. Ibrahim. Dielectric Based Sensing System for Banana Ripeness Assessment. *International Journal of Environmental Science and Development*, 5(3):286—289, 2014.
22) Jajang Juansah, I. Wayan Budiastra, Kiagus Dahlan, Kudang Boro Seminar. Electrical behavior of Garut citrus fruits during ripening: Changes in resistance and capacitance models of internal fruits. *Int. J. Eng. & Technol*, 12(04):1—8, 2012.
23) Anna Kicherer, Katja Herzog, Michael Pflanz, Markus Wieland, Philipp Rüger, Steffen Kecke, Heiner Kuhlmann, Reinhard Töpfer. An Automated Field Phenotyping Pipeline for Application in Grapevine Research. *Sensors*, 15(3):4823—4836, 2015.
24) Xing Liu. Electrical impedance spectroscopy applied in plant physiology studies., 2006
25) Devanand L. Luthria, Sudarsan Mukhopadhyay, Long-Ze Lin, James M. 34Harnly. A Comparison of Analytical and Data Preprocessing Methods for Spectral Fingerprinting. *Applied Spectroscopy*, 65(3):250—259, 2011.
26) Isar Nejadgholi, Miodrag Bolic. A comparative study of PCA, SIMCA and Cole model for classification of bioimpedance spectroscopy measurements. *Computers in Biology and Medicine*, 63:42—51, 2015.
27) Isar Nejadgholi, Herschel Caytak, Miodrag Bolic, Izmail Batkin, Shervin Shirmohammadi. Preprocessing and parameterizing bioimpedance spectroscopy measurements by singular value decomposition. *Physiological Measurement*, 36(5):983—999, 2015.

28) S. O. Nelson, Samir Trabelsi. Dielectric spectroscopy measurements on fruit, meat, and grain. *Trans. ASABE*, 51(5):1829—1834, 2008.
29) Bernt Jørgen Nordbotten. Bioimpedance Measurements Using the Integrated Circuit AD5933, 2008.
30) M D O'Toole, L A Marsh, J L Davidson, Y M Tan, D W Armitage, A J Peyton. Non-contact multi-frequency magnetic induction spectroscopy system for industrial-scale bio-impedance measurement. *Measurement Science and Technology*, 26(3):035102, 2015.
31) Uwe Pliquett. Bioimpedance: A Review for Food Processing. *Food Engineering Reviews*, 2(2):74—94, 2010.
32) Timothy W. Randolph. Scale-based normalization of spectral data. *Cancer Biomarkers*, 2(3, 4):135—144, 2006.
33) Mahfoozur Rehman, Basem A.J.A. Abu Izneid, Mohd Zaid Abdullah, Mohd Rizal Arshad. Assessment of quality of fruits using impedance spectroscopy. *International Journal of Food Science & Technology*, 46(6):1303—1309, 2011.
34) Graham B. Seymour, Natalie H. Chapman, Bee L. Chew, Jocelyn K. C. Rose. Regulation of ripening and opportunities for control in tomato and other fruits. *Plant Biotechnology Journal*, 11(3):269—278, 2013.
35) Mitar Simic. Realization of Complex Impedance Measurement System Based on the Integrated Circuit AD5933. *Telecommunications Forum (TELFOR), 2013 21st*:573—576, 2013.
36) M. Soltani, R. Alimardani, M. Omid. Prediction of banana quality during ripening stage using capacitance sensing system. *Australian Journal of Crop Science*, 4(6):443, 2010.
37) Christian Tronstad, Are Hugo Pripp. Statistical methods for bioimpedance analysis. *Journal of Electrical Bioimpedance*, 5(1), 2014.
38) Bradley Worley, Robert Powers. Multivariate analysis in metabolomics. *Current Metabolomics*, 1(1):92—107, 2013.
39) Sicong Zheng. An investigation on electrical properties of major constituents of grape must under fermentation using electrical impedance spectroscopy. 2009.
40) Resistors and Capacitors in Parallel — Department of Chemical Engineering and Biotechnology. Available: http://www.ceb.cam.ac.uk/research/groups/rg-eme/teaching-notes/resistors-and-capacitors-in-parallel.
41) [Nadia Arumugam,. 2012. "UN Says Europe Wastes 50% Of Fruit And Vegetables -- And America Isn't Much Better." http://www.forbes.com/sites/nadiaarumugam/2012/10/04/un-says-europe-wastes-50-of-fruit-and-vegetables-and-america-isnt-much-better/#53abe8947075 “[date visited: 29/10/2016].
42) Eriksson, L., et al., Introduction to Multi- and Megavariate Data Analysis using Projection Mathods (PCA&PLS).1999: Umetrics.